



**Sara da Costa Cabral
Pires Carvalho**

**Interacções entre Receptores Tirosina Cinase em
cancros humanos.**

**Receptor Tyrosine Kinases interactions in human
cancers.**



**Sara da Costa Cabral
Pires Carvalho**

**Interações entre Receptores Tirosina Cinase em
cancros humanos.**

**Receptor Tyrosine Kinases interactions in human
cancers.**

Dissertação apresentada à Universidade de Aveiro para cumprimento dos requisitos necessários à obtenção do grau de Mestre em Biologia Molecular e Celular, realizada sob a orientação científica da Doutora Paula Soares, IPATIMUP, Professora Auxiliar da Faculdade de Medicina da Universidade do Porto e do Doutor António Correia, Professor Associado com agregação do Departamento de Biologia da Universidade de Aveiro.

o júri

presidente

Prof.^a. Doutora Maria de Lourdes Gomes Pereira
Professora Associada com Agregação da Universidade de Aveiro

Prof. Doutor Fernando Carlos de Landér Schmitt
Professor Associado da Faculdade de Medicina da Universidade do Porto

Prof.^a. Doutora Ana Paula Soares Dias Ferreira
Professora Auxiliar da Faculdade de Medicina da Universidade do Porto

Prof. Doutor António Carlos Matias Correia
Professor Associado com Agregação da Universidade de Aveiro

agradecimentos

À Doutora Paula Soares, pela confiança em mim depositada, pela orientação, disponibilidade e entusiasmo colocados neste trabalho. Obrigada por me ter dado a oportunidade de trabalhar no IPATIMUP, centro de investigação de excelência.

Ao Professor Doutor Manuel Sobrinho Simões, por partilhar o seu vasto conhecimento com todos nós, é um privilégio ter a oportunidade de aprender consigo.

À Maria Oliveira, muito obrigada pela ajuda, dedicação e amizade. É um privilégio poder trabalhar e aprender contigo.

À Doutora Fernanda Milanezi, por toda a amizade e ajuda dispensada.

Ao Doutor Fernando Schmitt, obrigada pela possível colaboração.

Ao grupo do Cancer Biology, em especial a todos os da “tiróide”.

Ao grupo da “mama” obrigada pela disponibilidade.

À minha família, em especial aos meus pais e avós, um grande obrigada por todo o apoio e amizade.

Ao Márcio um obrigada muito especial pela tua amizade e amor. Obrigada por estares sempre “lá”.

palavras-chave

MET, ErbB-2, Cancro, Cancro da Mama, Cancro da Tiróide, PLA.

resumo

Objectivos: Os receptores tirosina cinase MET, ErbB-2 e EGFR foram identificados como tendo um papel importante no desenvolvimento e progressão de cancro. O objectivo deste estudo foi determinar a expressão e procurar interações dos receptores MET, ErbB-2 e EGFR em linhas celulares de carcinomas de tiróide e mama, e em tumores mamários.

Métodos: Neste estudo a expressão e interações dos receptores MET, ErbB-2 e EGFR foi determinada em duas linhas celulares de carcinoma da tiróide (TPC-1 e 8505C) e em duas linhas celulares de carcinomas da mama (MDA-MB-231 e SkBr3). A expressão de MET foi também estudada, por Imunohistoquímica, numa série de 219 carcinomas invasivos da mama, em microarrays, com um acompanhamento dos pacientes de 13 anos.

Resultados: Observámos que MET, ErbB-2 e EGFR são expressos em todas as linhas de tiróide e mama, e observámos também interações entre MET e ErbB-2. Na série de tumores mamários a expressão de MET foi significativamente relacionada com factores de prognóstico bem estabelecidos como ErbB-2, receptor de estrogénio, grau histológico e subtipos moleculares, sendo também significativamente associada com a diminuição da sobrevivência das pacientes. Por análise multivariada MET demonstrou ter um valor prognóstico independente.

Conclusões: O nosso estudo sugere que a comunicação entre MET e ErbB-2 pode ter um importante impacto clínico-patológico e que merece uma futura investigação, nomeadamente ao nível do desenvolvimento de novas terapêuticas.

keywords

MET, ErbB-2, Cancer, Breast cancer, Thyroid cancer, PLA.

abstract

Aims: Receptor tyrosine kinases (RTKs) MET, ErbB-2 and EGFR have been identified to play an important role in cancer development and progression. Our aim was to determine MET, ErbB-2 and EGFR expression and search for their interactions in thyroid and breast carcinoma-derived cell lines and human breast tumours.

Methods: We have studied the RTKs expression and interactions in two thyroid carcinoma-derived cell lines (TPC-1 and 8505C) and in two breast carcinoma-derived cell lines (MDA-MB-231 and SkBr3). We have also studied, by Immunohistochemistry, MET expression on a series of 219 invasive breast carcinomas with 13-year disease follow, using tissue-microarray.

Results: We observed that MET, ErbB2 and EGFR were expressed in both thyroid and breast cell lines, and we found physical interactions between MET and ErbB2. In the series of breast tumours, MET expression was significantly correlated with established prognostic factors such ErbB-2, oestrogen receptor (ER), grade and subtype, and was also significantly associated with poor clinical outcome of the patients. By multivariate analysis MET showed to have an independent prognostic value.

Conclusions: Our study suggests that the cross-communication between MET, and ErbB-2 may have clinicopathological impact and deserves further analysis namely in the design of novel combined therapeutic approaches.

Table of Contents

Table of Contents	XI
Abbreviations	XIII
List of Figures	XV
List of Tables	XIX
Introduction	1
Receptor Tyrosine Kinases	1
Epidermal Growth Factor Receptor family /ErbB Family	2
Epidermal Growth Factor Receptor	5
ErbB2	6
Hepatocyte Growth Factor receptor family	7
Thyroid cancer and RTKs	9
Breast cancer and RTKs	11
Aims	13
 Materials and methods	 15
Cell culture	15
Tissue Samples	15
Protein extraction and quantification	16
Co-Immunoprecipitation (Co-IP)	16
Small interfering RNA (siRNA) for MET downregulation	17
SDS-PAGE and Western Blotting analysis	18
Immunofluorescence	20
Proximity Ligation Assay	21
Immunohistochemistry	24
Statistical analysis	26

Results	27
Expression of MET, ErbB-2 and EGFR in carcinoma-derived cell lines	27
MET in Tissue Samples	33
Discussion	39
Conclusions	43
Bibliography	45
Annexes	53

Abbreviations

ATC	Anaplastic Thyroid Carcinoma;
ATP	Adenosine Triphosphate;
Co-IP	Co-Immunoprecipitation;
EGF	Epidermal Growth Factor;
EGFR	Epidermal Growth Factor Receptor;
ER	Oestrogen Receptor;
ErbB-2 OE	ErbB-2 Overexpression;
FTC	Follicular Thyroid Carcinoma;
HGF	Hepatocyte Growth Factor;
HGFR	Hepatocyte Growth Factor Receptor;
MAPK pathway	Mitogen-Activated Protein Kinase pathway;
MET	Mesenchymal Epithelial Transition factor;
NSCLC	Non-small Cell Lung Carcinoma;
PR	Progesterone Receptor;
PDTC	Poorly Differentiated Thyroid Carcinoma;
PI3K pathway	Phosphatidylinositol 3-kinase pathway;
PLA	Proximity Ligation Assay;
PTC	Papillary Thyroid Carcinoma;
RCA	Rolling Circle Amplification;
RTK	Receptor Tyrosine Kinase;
SDS-PAGE	Sodium Dodecyl Sulfate – Poliacrylamide Gel Electrophoreses;
siRNA	Small interfering Ribonucleic Acid;
TKI	Tyrosine Kinase Inhibitor;
TMA_s	Tissue Microarrays;
TNC	Triple Negative Carcinoma;
TSH	Thyroid Stimulating Hormone;
WHO	World Health Organization.

List of figures

Figure 1: Human Receptor Tyrosine Kinases Family. The prototypic receptor for each family is indicated above the receptor, and the known members are listed below. Abbreviations: AB, acidic box; CadhD, cadherin-like domain; CRD, cysteine-rich domain; DiscD, discoidin-like domain; EGFD, epidermal growth factor-like domain; FNIII, fibronectin type III-like domain; IgD, immunoglobulin-like domain; KrinD, kringle-like domain; LRD, leucine-rich domain. RTK members in bold and italic type are implicated in human malignancies. (Adapted from Blume-Jensen & Hunter, 2001).

Figure 2: ErbB receptor activation — a structural view. The three-dimensional (3D) coordinates and a schematic representation of the extracellular and intracellular domains of ErbB receptors. The plasma membrane is represented by a purple arc. In the diagrams of the ectodomain, domain I is colored purple, domain II green, domain III red and domain IV dark blue. The ligand (EGF) is colored yellow. The dimerization loop, a part of domain II, is in orange. Left: before ligand binding, domains II and IV are connected through an intramolecular bond involving the dimerization loop, thereby preventing the formation of a high-affinity ligand binding site, which is composed of domains I and III. Middle: ligand binding induces major conformational changes and unmasks the dimerization. Right: receptor dimerization mediated by the exposed dimerization loops. In the diagrams of the intracellular domain, the N-lobe of the kinase domain is colored grey and the C-lobe cyan. Helix a-C is dark grey (adapted from Bublil & Yarden, 2007).

Figure 3: The ErbB signalling network. **a.** Ligands and the ten dimeric receptor combinations. Numbers in each ligand block indicate the respective high-affinity ErbB receptors. **b.** Signalling to the adaptor/enzyme layer, shown only for two receptor dimers, the weakly mitogenic EGFR homodimer and the relatively potent ErbB2/ErbB3 heterodimer. **c.** How the signals are translated to specific types of output. (Adapted from Yarden & Sliwkowski, 2001).

Figure 4: MET pathway. HGF binds to the extracellular domain of MET, which induces tyrosine kinase activity, transducing intracellular signalling through a cascade of mediators (ovals). This results in up-regulation of several transcription factors producing altered cellular physiology (pale blue boxes) with salutary effects on disease endpoints (dark blue boxes). Adapted from www.angion.com/science.asp

Figure 5. Schematic representation of the histological features of follicular cell derived tumours. Abbreviations: NT, normal thyroid; PTC, papillary thyroid carcinoma; FVPTC, follicular variant of papillary thyroid carcinoma; FTC, follicular thyroid carcinoma; ATC, anaplastic thyroid carcinoma.

Figure 6: Schematic presentation of Proximity Ligation Assay method adapted from Duolink PLA User Manual.

Figure 7: MET (145 kDa), EGFR (170 kDa) and ErbB-2 (185 kDa) are present in both thyroid (TPC-1 and 8505C) and breast (MDA-MB-231 and SkBr3) cell lines. Whole cell lysates from TPC-1, 8505C, MDA-MB-231 and SkBr3 were separated by SDS-PAGE and analysed for MET, EGFR and ErbB-2 expression by Western Blot. Actin was used as loading control.

Figure 8: MET, EGFR and ErbB-2 are present in both thyroid (TPC-1 and 8505C) and breast (MDA-MB-231 and SkBr3) cell lines (400x). The MET, EGFR and ErbB-2 are stained green (FITC) and the nuclei are stained blue (DAPI).

Figure 9: MET interacts with ErbB-2, but not with EGFR in TPC-1 (A), 8505C (B), MDA-MB-231(C) and SkBr3 (D). Immunoprecipitation with IgG mouse was used as a negative control in each experiment.

Figure 10: The MET- ErbB-2 interaction in the 8508C cell line by PLA technique is shown (as an example of PLA results). A – Fluorescence microscope image, the nuclei are stained in blue and the hybridization signals in red (400x). B (inset) – Overlay between images from the fluorescent microscope and the software analysis scheme.

Figure 11: MET and ErbB-2 interactions in TPC-1, 8505C, MDA-MB-231 and SkBr3 cell lines, analysed by Proximity Ligation Assay. The histograms indicate the number of MET and ErbB-2 interactions (residual control values are not always visible). CN, negative control.

Figure 12: Western blot analysis of MET, ErbB-2, Erk1/2 activation in TPC-1 (A), MDA-MB-231 (B), and SkBr3 (C) cells after MET down-regulation. Actin was used as control. 1. Control cells (no treatment); 2. Control cells treated only with Lipogen; 3. Control cells treated with scramble RNA oligonucleotides; 4. Cells treated with MET siRNA.

Figure 13: MET and ErbB-2 interactions analysed by Proximity Ligation Assay in TPC-1, MDA-MB-231 and SkBr3 cell lines after MET downregulation. The histograms indicate the number of MET and ErbB-2 interactions (negative control residual values not always visible). The dark shade histograms demonstrate the MET and ErbB-2 interactions in the cell lines without MET downregulation. CN, negative control.

Figure 14: Immunohistochemical staining of MET in two different breast cancer tissues (400x). MET membranar expression considered as positive staining is indicated by blue arrows.

Figure 15: Kaplan-Meier analysis of disease-related survival demonstrates that the presence of MET tend to increase a worse prognosis and an earlier death. Statistical significance was assessed using the Log-rank test.

Figure 16: Kaplan-Meier analysis of disease-related survival in Luminal (A), ErbB-2 OE (B) and Triple negative (C) subtypes of tumours. Statistical significance was assessed using the Log-rank test.

List of Tables

Table 1: Primary antibodies and respective incubation conditions used for WB analysis.

Table 2: Primary antibodies and respective incubation conditions used for Immunofluorescence analysis.

Table 3: Primary antibodies for the interactions used for Proximity Ligation Assay.

Table 4: Immunohistochemical classification.

Table 5: Statistical comparison between the presence/absence of MET and the clinicopathologic characteristics of breast cancer.

Table 6: Univariate analysis of the clinicopathologic factors for the 13-year disease-related survival.

Table 7: Multivariate analysis of the 13-year disease-related survival using only the statistically significant clinicopathologic factors from the univariate analysis.

Introduction

Receptor tyrosine kinases

Receptor tyrosine kinases (RTKs) are cell-surface allosteric enzymes, a subclass of transmembrane-spanning receptors with an extracellular ligand binding domain, a transmembrane domain and an intracellular tyrosine kinase domain.

The tyrosine kinase activity is promoted by extracellular ligand binding. This binding induces a noncovalent oligomerization, mostly dimerization of monomeric receptors that will lead to the autophosphorylation of tyrosines in the carboxyl terminal segment. Once activated, the receptor recruits other molecules that function as docking sites for downstream signal transduction molecules (Blume-Jensen & Hunter, 2001).

The RTKs are the high affinity cell surface receptors of many ligands such as polypeptide growth factors, cytokines and hormones that activate intracellular pathways which regulate cell division activity, differentiation and morphogenesis.

More than half of the known RTKs have been repeatedly found either mutated or overexpressed in human malignancies. In fact, more than 70% of the known oncogenes and proto-oncogenes involved in cancer code for tyrosine kinases.

Oncogenic receptor tyrosine kinases induce inappropriate activation of downstream signalling components that leads to enhanced cell proliferation and increased cell survival, through the mitogenic and survival pathways respectively (Krauss, G., 2003).

There are 58 transmembrane RTKs identified thus far, classified in 20 different families (Robinson *et al.*, 2000) (Figure 1).

This work is focus on the Epidermal Growth Factor (EGF) and Hepatocyte Growth Factor (HGF) receptors families.

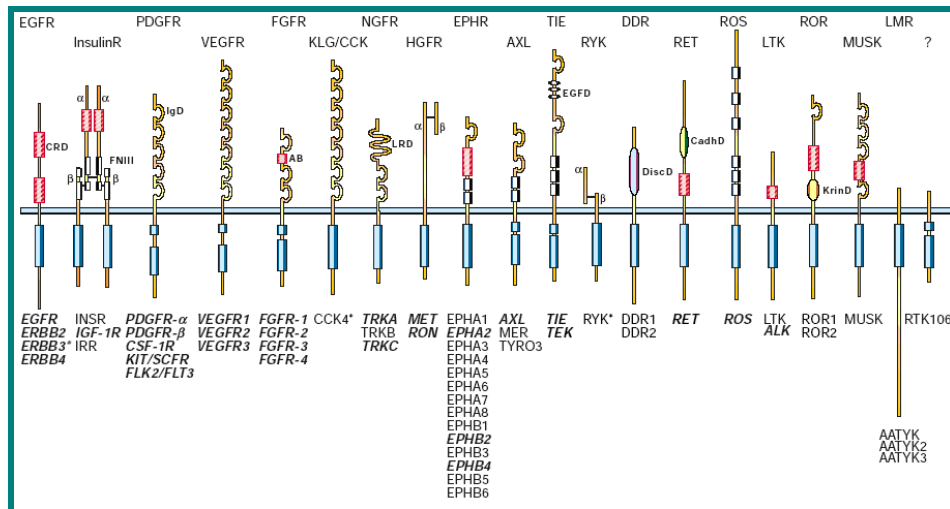


Figure 1. Human Receptor Tyrosine Kinases Family. The prototypic receptor for each family is indicated above the receptor, and the known members are listed below. Abbreviations: AB, acidic box; CadhD, cadherin-like domain; CRD, cysteine-rich domain; DiscD, discoidin-like domain; EGFD, epidermal growth factor-like domain; FNIII, fibronectin type III-like domain; IgD, immunoglobulin-like domain; KrinD, kringle-like domain; LRD, leucine-rich domain. RTK members in bold and italic type are implicated in human malignancies. (Adapted from Blume-Jensen & Hunter, 2001).

Epidermal Growth Factor Receptor family /ErbB Family

The subclass I of the RTKs superfamily consists of the ErbB or EGF Receptors and comprises 4 structurally related members: EGFR/ErbB1/HER1, ErbB2/HER2/neu, ErbB3/HER3 and ErbB4/HER4. All ErbB members have in common an extracellular ligand binding cystein-rich domain, a single membrane-spanning region, and a cytoplasmic protein tyrosine kinase containing domain (Hynes & Lane, 2005).

Under normal physiological conditions, the activation of the ErbB receptors is controlled by a spatial and temporal expression of their ligands, members of the EGF-related peptide growth factor family. Each ErbB receptor is an inactive monomer that dimerizes, in different homo- and heterodimers, in response to ligand binding.

The ErbB family of ligands can be divided in three groups, comprising 11 members: the first includes EGF, transforming growth factor- α (TGF- α) and amphiregulin, all three binding specifically to EGFR; the second group includes betacellulin, heparin-binding EGF (HB-EGF) and epiregulin, which bind either to EGFR and ErbB4; the third group is composed of neuregulins (NRGs) and it is subdivided into two subgroups based on their capacity to bind ErbB3 and ErbB4 (NRG1 and NRG2) or only to ErbB4 (NRG3 and NRG4) (Hynes & Lane, 2005).

Two out of the four ErbB proteins, namely EGFR and ErbB4, are autonomous, when bound by a ligand they undergo dimerization and generate intracellular signals. The other two receptors are non-autonomous. ErbB2 do not bind to soluble ligands, however acts as a preferred partner in heterodimeric complexes with other ligand bound ErbBs. ErbB3 cannot generate signals because the kinase function on this receptor is impaired. Nevertheless, in the context of a heterodimer, primarily with ErbB2, ErbB3 can enhance potent intracellular signals (Bublil & Yarden, 2007).

The extracellular region of each ErbB receptor consists of four domains I-IV (Figure 2). It was shown that the domains I and III are essential for peptide binding, that the direct receptor-receptor interaction is induced by domain II (dimerization arm), and that ligands are not involved in this receptor-receptor interaction (Hynes & Lane, 2005).

When EGFR or ErbB3 are free of ligand they assume a tethered structure and the domain II is blocked by intramolecular interactions between domains II-IV. The structure of ErbB2 extracellular region is radically different due to have a fixed conformation that resembles the ligand-activated state: the domain II-IV interaction is absent and the dimerization loop in domain II is exposed, explaining why this receptor is the preferred partner for the other activated ErbBs.

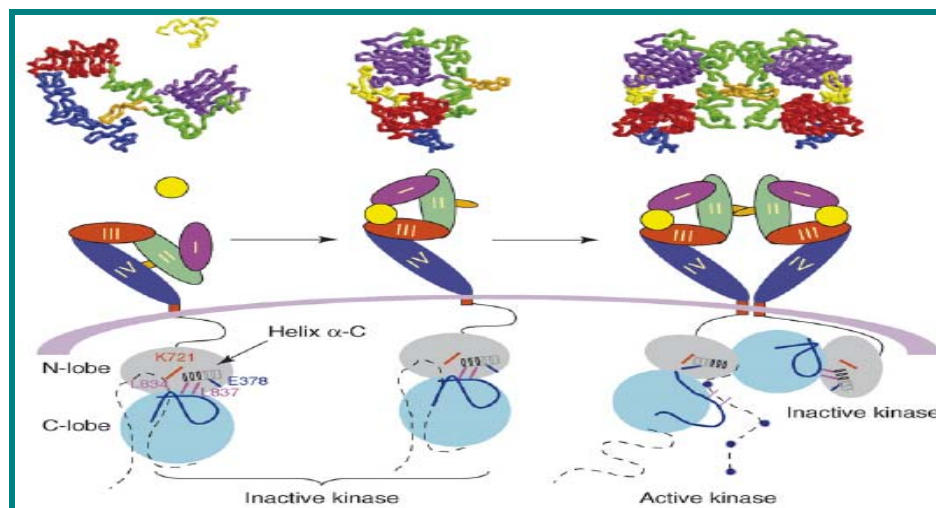


Figure 2. ErbB receptor activation — a structural view. The three-dimensional (3D) coordinates and a schematic representation of the extracellular and intracellular domains of ErbB receptors. The plasma membrane is represented by a purple arc. In the diagrams of the ectodomain, domain I is colored purple, domain II green, domain III red and domain IV dark blue. The ligand (EGF) is colored yellow. The dimerization loop, a part of domain II, is in orange. Left: before ligand binding, domains II and IV are connected through an intramolecular bond involving the dimerization loop, thereby preventing the formation of a high-affinity ligand binding site, which is composed of domains I and III. Middle: ligand binding induces major conformational changes and unmasks the dimerization. Right: receptor dimerization mediated by the exposed dimerization loops. In the diagrams of the intracellular domain, the N-lobe of the kinase domain is colored grey and the C-lobe cyan. Helix α -C is dark grey (adapted from Bublil & Yarden, 2007).

Two of the main pathways activated by the receptors are the Mitogen-Activated Protein Kinase (MAPK) and the Phosphatidylinositol 3-kinase (PI3K) pathway (Figure 3).

The MAPK pathway is involved in all ErbB-receptor activations, and the PI3K pathway is triggered downstream of most active dimers. For example, whereas PI3K couples directly with ErbB3 and ErbB4, it does so indirectly with EGFR and ErbB2, via an intermediary adaptor protein known as Cbl, as a result the potency and kinetics of this pathway activation differ from the MAPK pathway (Yarden & Sliwkowski, 2001).

The ErbB signalling system comprises a highly complex and interactive “multilayered” network. Signals are initiated at the cell surface where ligand-receptor interactions take place, and the resulting receptor dimerization and activation relays and amplifies the signal through an intricate cytoplasmic system of enzymes, proteins, and small-molecule secondary messengers. This process of signal transduction culminates in the nucleus where gene control and protein transcription are modified, producing effects on key cellular regulatory processes, such as differentiation, adhesion, growth, migration, and apoptosis (Mass, R. 2003).

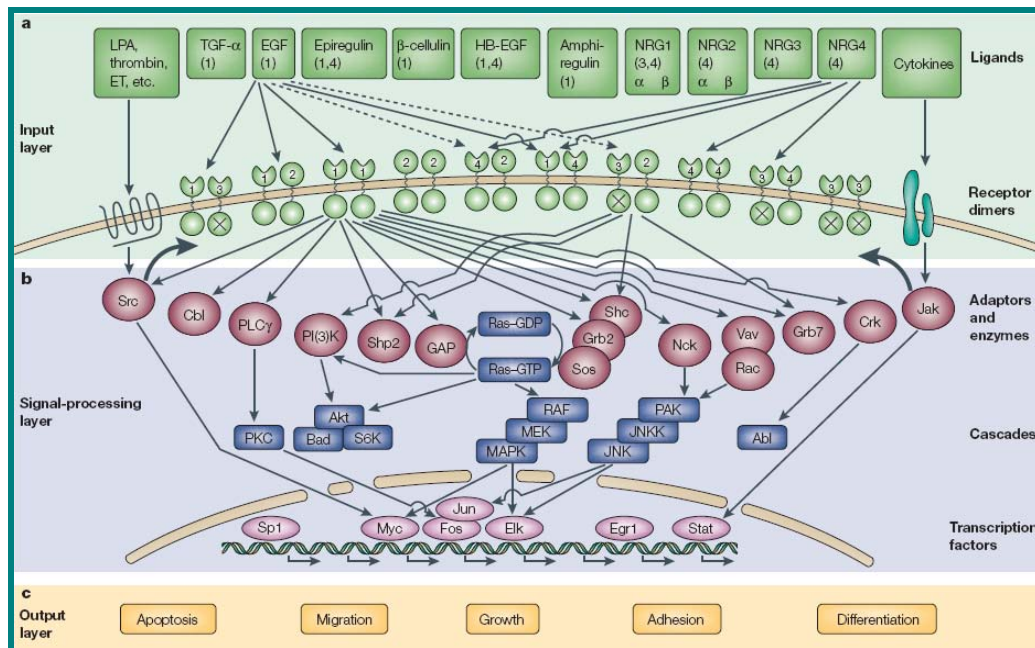


Figure 3. The ErbB signalling network. **a.** Ligands and the ten dimeric receptor combinations. Numbers in each ligand block indicate the respective high-affinity ErbB receptors. **b.** Signalling to the adaptor/enzyme layer, shown only for two receptor dimers, the weakly mitogenic EGFR homodimer and the relatively potent ErbB2/ErbB3 heterodimer. **c.** How the signals are translated to specific types of output. (Adapted from Yarden & Sliwkowski, 2001).

Aberration of ErbB family receptors function is implicated in major pathologies, such as cancer or neurodegenerative diseases. It is well documented that excessive ErbB

signalling, arising from receptor overexpression, mutations or autocrine stimulation, is a characteristic of a wide variety of solid tumours like neoplasms of the brain, breast, lung, ovary, pancreas, prostate and thyroid. As an example, high EGFR expression was found in the majority of carcinomas, and amplification of ErbB2 gene can be found in 20-30% of metastatic breast lesions. As a consequence, ErbB receptors are attractive candidates for targeted therapy. In fact, several anti-ErbB monoclonal antibodies and small molecule tyrosine kinase inhibitors (TKIs) are currently under investigation, or have been already licensed, like Gefitinib for EGFR and Trastuzumab for ErbB2 (Bublil & Yarden, 2007).

Epidermal Growth Factor Receptor

Epidermal Growth Factor Receptor (EGFR) is the first member of the ErbB receptor family. This receptor is a 170 kDa transmembrane cell surface glycoprotein encoded by the ErbB proto-oncogene located on the chromosome 7 at p12.3-12.1.

The ErbB receptors are implicated in the development of many types of cancer, being EGFR the first tyrosine-kinase receptor to be linked directly to human tumours (Schiff *et al.*, 2004).

Activation of the proto-oncogene encoding EGFR contributes to cellular transformation and provides to tumour cells substantial growth and survival advantages. High levels of this receptor and its ligands have been recognized as a common component of several cancer types, including bladder, breast, colon, head and neck, lung carcinomas and gliomas.

Aberrant EGFR activation, which is mediated through gene amplification, mutations and autocrine stimulation, appears to be an important factor in tumourigenesis as well as an essential driving force for the aggressive growth behaviour of cancer cells and poor prognosis. Its activation contributes to several other tumourigenic mechanisms including tumour survival, invasion, resistance to apoptosis, angiogenesis and metastatic spread (Ensinger *et al.*, 2004).

The high frequency of abnormalities in EGFR signalling in human carcinomas and gliomas together with laboratory and clinical studies showing that inhibition of this receptor can

impair tumour growth indicate this receptor as an attractive target for the development of cancer therapeutics (Dancey & Freidlin, 2003).

Several small molecule inhibitors of EGFR are currently in use to treat non-small cell lung carcinoma (NSCLC) patients, like Gefitinib (Iressa) and Erlotinib (Tarceva), or in clinical trials. These inhibitors disrupt EGFR kinase activity by binding the adenosine triphosphate (ATP) pocket within the catalytic domain, inhibiting downstream signalling, thus preventing tumour-cell proliferation and angiogenesis, inducing apoptosis. Furthermore, additive or synergistic cytotoxic effects are observed on tumour cells when used in combination with standard cancer therapies (Guo *et al.*, 2008). The response rates to any EGFR inhibitor are strongly associated with the presence of somatic mutations within the tyrosine kinase domain of the receptor. In this way only a subfraction of patients with tumours dependent on EGFR for growth and survival respond clinically to EGFR inhibitors (Mitsiades *et al.*, 2007).

ErbB2

ErbB2 is the second member of ErbB family. This receptor is a 185 kDa transmembrane cell surface glycoprotein encoded by the *ErbB-2* proto-oncogene located on the chromosome 17 at q21.2 (Kremser *et al.*; 2003).

ErbB2 is the preferred partner of the ligand bound EGFR, ErbB3 and ErbB4 for the formation of catalytically active heterodimers. From these complexes, the ErbB2/ErbB3 heterodimers are more stable and consequently have a more potent signalling (Pinkas-Kramarski *et al.*; 1998).

It is known that normal human cells constitutively express a small amount of ErbB2 protein in the plasma membrane. The overexpression of this receptor in pathological conditions is usually due to gene amplification, being originally detected in breast tumours (Freudenberg *et al.*; 2005). Lately, was shown that ErbB-2 overexpression is found in a wide range of human carcinomas originated in different organs such bladder, colon, pancreas, lung, ovary and stomach (Ménard *et al.*; 2003). Overexpression leads to an increase of tumourigenicity, tumour invasiveness, increased metastatic potential, and altered sensitivity to hormonal and chemotherapeutic agents (Freudenberg *et al.*; 2005).

Mutations in the kinase domain of *ErbB-2* proto-oncogene were recently identified. According to Stephens *et al.*, 2004, three unambiguous somatic mutations were identified in primary NSCLC: two in-frame insertions and a missense substitution. In this study two other likely somatic mutations, corresponding to two different in-frame insertions, were also detected in two additional tumours, all located in the kinase domain, however no normal tissue was available to compare. It was also shown that the ErbB-2 immunohistochemical staining revealed no differences between tumours with or without mutations, indicating that the overexpression probably does not accompany the mutation. In addition three further somatic mutations were found, one in a glioblastoma, one in a gastric tumour and other in an ovarian tumour, all of them in the kinase domain.

In the NSCLC the ErbB-2 mutations were located in the exons 19 and 20, point mutations and in-frame insertions respectively, also in the kinase domain (Willmore-Payne *et al.*; 2006). In an hepatocarcinoma a single novel missense somatic mutation was found, occurring in the activation domain, which alters a basic hydrophilic residue to an acidic hydrophilic residue, this mutation is expected to affect the activation domain function (Bekaii-Saab *et al.*; 2006).

Hepatocyte Growth Factor receptor family

The HGFR family is structurally distinct from others RTK families. *MET*, *RON* and *SEA* are the known proto-oncogenes of this family coding for receptors.

Mesenchymal Epithelial Transition factor receptor (MET) is the only high affinity receptor known for Hepatocyte Growth Factor (HGF), a multifunctional cytokine stimulating cell proliferation, motility and extracellular matrix invasion (Wasenius *et al.*, 2005).

MET is encoded by *MET* proto-oncogene, located in the chromosome 7 at q31-34, is a single pass cell membrane glycoprotein dimeric molecule composed of a 50KDa α chain disulfide-linked to a 145KDa β chain in a $\alpha\beta$ complex of 190KDa. The α chain is exposed at the cell surface and the β chain spans the plasma membrane, both α and β subunits are necessary for the biological activity. The intracellular domain of this receptor includes a divergent juxtamembrane region followed by a conserved tyrosine kinase catalytic domain

and a C-terminal sequence, which is responsible for receptor coupling to intracellular transducers (Longati *et al.*, 2001).

MET and its ligand HGF are expressed in a variety of tissues, and their expression is normally confined to cells of epithelial and mesenchymal origin, respectively. The transduction of signalling of HGF by MET and subsequent biologic effects has been shown to be important in epithelial-mesenchymal interaction and regulation of cell migration, motility, cell proliferation and survival, angiogenesis, morphogenic differentiation, and organization of three-dimensional (3D) tubular structures (e.g. renal tubular cells and gland formation) during development and tissue repair.

At molecular level, binding of HGF to the MET extracellular ligand-binding domain results in receptor multimerization and trans-phosphorylation of multiple tyrosine residues at the intracellular region. Tyrosine phosphorylation at MET juxtamembrane, catalytic, and cytoplasmic tail domains regulate the internalization, catalytic activity, and docking of regulatory substrates, respectively. Activation of MET leads to the binding and phosphorylation of adaptor proteins such as Gab-1, Grb2, Shc, and c-Cbl and subsequent activation of signal transducers such as PI3K, PLC- γ , STATs, ERK 1 and 2, and FAK (Christensen *et al.*, 2004) (Figure 4).

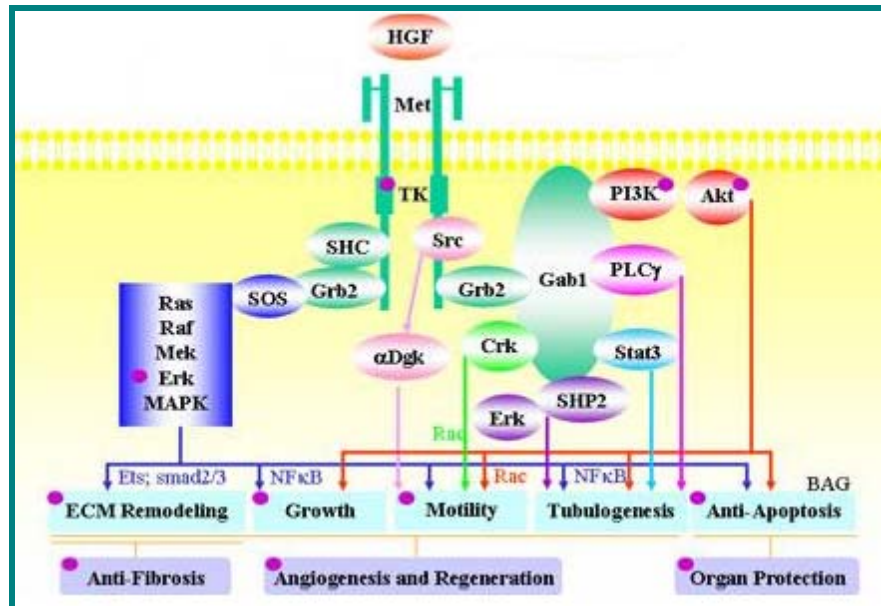


Figure 4. MET pathway. HGF binds to the extracellular domain of MET, which induces tyrosine kinase activity, transducing intracellular signalling through a cascade of mediators (ovals). This results in up-regulation of several transcription factors producing altered cellular physiology (pale blue boxes) with salutary effects on disease endpoints (dark blue boxes). Adapted from www.angion.com/science.asp

The first alteration of the *MET* gene was identified in a chemically treated DNA-transfected human osteosarcoma cell line. In subsequent studies, amplifications of *MET* have been demonstrated in colorectal cancer, point mutations have been specifically associated with papillary carcinoma of the kidney, and overexpression has been demonstrated in a variety of epithelial tumours, including papillary carcinoma of the thyroid (Ruco *et al.*, 2001).

Deregulated activation of MET can induce tumour-invasive growth into the surrounding tissues and penetration into the vasculature. Some studies propose that *MET* mutations are common in cancer metastasis, suggesting a role in metastasis formation (DiRenzo *et al.*, 2000).

The interactions between MET and EGFR proteins, and MET and ErbB-2 proteins in cancer are beginning to be studied. In 2000 Bergstrom *et al.*, have shown that the presence of an autocrine activation of the EGFR in several thyroid carcinoma cell lines resulted in an increased MET expression and activity, indicating a cross-communication between the two growth factor receptors signalling pathways. In NSCLC this relationship was also documented by Guo *et al.*, 2007 and Agarwal *et al.*, 2009. A recent study from Shattuck *et al.*, 2008 reports that MET is frequently expressed in ErbB2 overexpressing breast cancer cells. Importantly, Shattuck *et al.* observed in a *in vitro* model that MET contributes to Trastuzumab (monoclonal antibody against ErbB2) resistance, whereas MET activation protects cells against Trastuzumab action by abrogating p27 induction. Remarkably, ErbB2 overexpression breast cancer cells rapidly up-regulate MET expression after Trastuzumab treatment, promoting their own resistance and suggesting that a subset of ErbB2 overexpression patients may benefit from combined inhibition of ErbB2 and MET.

Thyroid cancer and RTKs

Although tumours of thyroid account for only 1% of the overall human cancer burden, it is the most prevalent type of endocrine malignancy. This type of cancer occurs primarily in young and middle aged women's, with approximately 122,000 new cases per year worldwide.

Thyroid carcinomas can be caused by environmental, genetic and hormonal factors and comprise a heterogeneous group of neoplasms with distinctive clinical and pathological characteristics (DeLellis, R. 2006). Because of the thyroid dependence on environmental iodine, it is particularly vulnerable to the radioactive iodine effects and to thyroid stimulating hormone (TSH) stimulation resulting from iodine deficiency (DeLellis *et al.*, 2004).

According to the World Health Organization (WHO) classification of tumours, the main histological types of thyroid carcinomas are characterized on the basis of histological and clinical parameters.

Follicular cell derived carcinomas are divided into well-differentiated, poorly differentiated (PDTC) and undifferentiated or anaplastic types (ATC) (Figure 5). The well-differentiated carcinomas are subdivided in Papillary (PTC), which accounts for about 80% of all thyroid carcinomas, and Follicular (FTC) carcinomas. The vast majority of follicular cell derived tumours are indolent neoplasms. Nevertheless anaplastic thyroid carcinomas are among the most aggressive of all human malignancies with a high mortality and a mean survival of 6 months after the diagnosis.

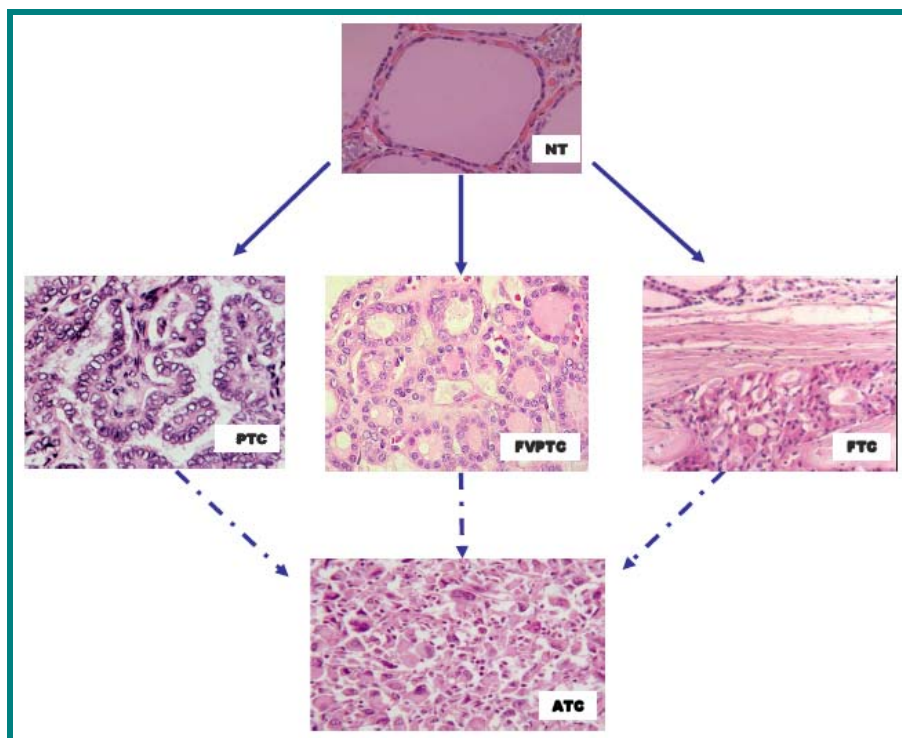


Figure 5. Schematic representation of the histological features of follicular cell derived tumours. Abbreviations: NT, normal thyroid; PTC, papillary thyroid carcinoma; FVPTC, follicular variant of papillary thyroid carcinoma; FTC, follicular thyroid carcinoma; ATC, anaplastic thyroid carcinoma.

The expression and the role of EGFR in thyroid carcinomas is still controversial and yet to be clarified. In some preclinical studies EGF has been shown to stimulate follicular cell proliferation and to enhance the migration and invasiveness of papillary thyroid cancer cells. The literature generally supports that EGFR have a low expression in the normal thyroid tissue but is overexpressed in anaplastic and papillary thyroid carcinomas (Schiff *et al.*, 2004). Other studies, such as Mitsiades *et al.*, 2007, consider that EGFR is usually not overexpressed or overactivated in thyroid carcinomas compared with adjacent non-malignant thyroid tissue.

Also the role played by ErbB2 in thyroid carcinomas is still controversial. Several studies were performed examining the expression of this protein in thyroid carcinomas, leading to conflicting results (Freudenberg *et al.*; 2005). In papillary carcinoma (and also in normal thyroid), ErbB-2 expression occurs mainly in the cytoplasm, possibly indicating an internalization of the ligand-receptor complex and its degradation. No mutations or amplification were referred (Soares *et al.*, 1994; Utrilla *et al.*, 1999; Gumurdulu *et al.*, 2003; Kremser *et al.*, 2003; Freudenberg *et al.*, 2005).

It is consistently reported that the MET protein is distinctly overexpressed in PTC. By immunohistochemistry the MET overexpression is well documented, being the expression levels of the protein low in normal thyroid tissue, thyroid adenomas, and in nonneoplastic thyroid diseases such Grave's and Hashimoto's diseases (Wasenius *et al.*, 2005). Protein overexpression was not associated with amplification or rearrangements of the *MET* gene and the MET protein produced by tumour cells did not show major structural alterations (Ruco *et al.*, 2001). Some authors suggest the possibility of a link between MET overexpression and RET rearrangements, which are detected in 20-50% of cases of PTC (Ivan *et al.*, 1997).

Breast cancer and RTKs

Breast cancer is a heterogeneous disease composed of a growing number of recognized biological subtypes. It encompasses a wide variety of pathological entities and a range of clinical behaviours. Its clinical signs, symptoms and prognosis depend largely on whether

the disease is confined or has metastasized to adjacent or distant parts of the body (Baselga & Norton, 2002).

Breast cancer has the highest incidence of all cancers in women, and according to the data from Portuguese League against Cancer (www.ligacontracancro.pt), breast cancer is the most frequently diagnosed cancer in Portuguese women, one in each ten Portuguese women will develop this disease during life, being diagnosed about 4.500 new cases per year.

Breast cancer classification can be approached from two main standpoints. The first is based on the histological appearance in combination grading system, in which grading includes proliferation rate, degree of differentiation and nuclear pleomorphism. The second approach is to classify breast cancers on the basis of a marker that can predict a probable response to a particular treatment, such as expression of hormone receptors (oestrogen and progesterone) and ErbB-2. At least 15% of breast cancers lack the expression of oestrogen receptors (ERs), progesterone receptors (PRs), and ErbB-2, being referred to as triple-negative cancers (TNCs). TNCs generally have a poor prognosis and are a heterogeneous group of cancers (Gusterson, 2009).

Expression profiling analyses using microarrays have demonstrated that breast cancers can be classified according to their expression patterns into three groups. Luminal, when they have the characteristics of luminal cells, Basal, when express genes usually expressed in normal basal/myoepithelial cells and ErbB2 overexpression (Kapp *et al.*, 2006, Milanezi *et al.*, 2008, Weigelt *et al.*, 2008).

Luminal carcinomas are currently subdivided into A and B. The luminal A have usually a low histological grade, an excellent prognosis and show high levels of expression of ER-activated genes. Luminal B carcinomas co-express ER and ErbB2 and show a higher histological grade, higher proliferation rates and a poorer prognosis than luminal A tumours. Basal-like carcinomas are ER and ErbB2 negative, and characteristically express Cytokeratin 5, 14 and 17, P-chaderin and EGFR. This group of carcinomas is reported to have a more aggressive clinical behaviour, and less significant response to conventional chemotherapy than luminal breast carcinomas. ErbB2 overexpressing tumours are associated with lack or reduced ER expression, overexpression of ErbB-2, and have very aggressive clinical behaviour (Milanezi *et al.*, 2008).

The role of EGFR in breast carcinogenesis is still poorly established. To date, there are no widely agreed criteria for analysis of EGFR status as a predictive or prognostic marker for this disease (Chan *et al.*, 2006). EGFR overexpression in 16-36% of breast cancers has been reported by Bhargava *et al.*, 2005. No *EGFR*-activating mutations were found.

The association of ErbB2 expression with cancer is best studied in breast carcinomas where the *ErbB-2* gene is amplified and overexpressed in about 20-30%, conferring a more aggressive behaviour, a significantly lower survival rate and a shorter time to relapse (Yarden & Sliwkowski, 2001; Menendez *et al.*, 2006; Palmieri *et al.*, 2007).

According to the few works available MET overexpression in breast cancer is associated with tumour progression and correlates with poor survival and decrease relapse-free. MET receptor overexpression is an independent predictor of poor prognosis in breast cancer (Bonine-Summers *et al.*, 2007; Garcia *et al.*, 2007; Lindermann *et al.*, 2007; Shattuck *et al.*, 2008).

Aims

The study of tyrosine kinase receptors has been a major issue in cancer research. However, most of the studies relay in the individual expression of RTKs. Assessment of RTKs gene expression and protein interactions not only improves the ability to diagnose and classify neoplasms, but also helps to design new therapeutic strategies.

Our general aim was to go ahead RTKs expression in order to evaluate putative receptor interactions in both thyroid and breast tumour models.

Specific aims

Evaluate the expression of ErbB-2, EGFR and MET in cell lines from two tumour models, specifically thyroid and breast cancer.

Characterize the interaction levels between ErbB-2, EGFR and MET, both in thyroid and breast cancers cell lines.

Explore in a human cancer model (human breast cancer) the biological and prognostic implications of MET expression and the relation between the expressions of the receptors.

Materials and Methods

Cell culture

Five human thyroid-derived cell lines were maintained in culture. Two cell lines derived from papillary thyroid carcinoma (PTC) – TPC-1 and K1, one derived from follicular thyroid carcinoma (FTC) – XTC-1 and two derived from undifferentiated thyroid carcinoma (UTC) – C643 and 8505C.

Three human breast carcinoma-derived cell lines were maintained in culture. The ErbB-2 overexpressing (ErbB-2 OE) subtype SkBr3 derived-cell line, the basal subtype MDA-MB-231 derived-cell line and the luminal A MCF-7 derived-cell line.

TPC1, C643 and 8505C cell lines were maintained in RPMI-1640 (GIBCO) with 10% fetal bovine serum (FBS) (GIBCO) and 1% Penicillin-Streptomycin (Pen-Strep) (GIBCO).

The K1 cell line was maintained in 2:1:1 Dulbecco's modified Eagle's medium (DMEM) (GIBCO), Ham's F-12 medium (GIBCO), MCDB104 supplemented with 10%FBS (GIBCO), 1% Pen-Strep (GIBCO), 1% L-Glutamine (GIBCO), 0.5% Sodium Pyruvate (NaPyr) (SIGMA) and 1.25% Sodium bicarbonate (NaHCO₃) (SIGMA).

The XTC-1 cell line was maintained in 1:1 DMEM:Ham's F12 medium (GIBCO) supplemented with 10%FBS (GIBCO), 1% Pen-Strep (GIBCO), 0.1% Insulin 10mg/ml (SIGMA), 0.5% TSH 2.00U/ml (SIGMA) and 0.5% Fungizone 250ng/ml (GIBCO).

All the three breast carcinoma-derived cell lines were maintained in 1X DMEM (GIBCO) with 10% FBS (GIBCO) and 1% Pen-Strep (GIBCO).

All the cell lines have adherent cell growth. The cells were incubated at 37°C in a humid atmosphere with 5% carbon dioxide.

Tissue Samples

A series of breast carcinomas collected by the Institute of Pathology from Araçatuba, Brazil, was provided by Prof. Fernando Schmitt from IPATIMUP. This series was composed by 219 invasive carcinomas in 23 Tissue Microarrays (TMAs), with a well

established follow-up, age and lymph node metastasis information. A classification by subtypes had been previously completed, being 138 Luminal, 21 ErbB-2 OE and 60 triple negative tumours, and a classification by grade was also performed, being 105 tumours grade I, 84 grade II and 30 grade III. All the most important markers of breast carcinomas had already been tested, such as ER, ErbB-2, PR, P-chaderin, P53, P63 and EGFR.

Protein extraction and quantification

Culture cells were lysated using Catenin lysis buffer and centrifuged at 14000rpm, 4°C for 15minutes. The supernatant was kept at -20°C.

Sample protein quantification was made by a colorimetric assay, based on the Bradford MM method, using the DC Protein Assay Kit (Bio-Rad). Bovine serum albumin (BSA) was used as standard, at several known concentrations (0%, 0.5%, 0.75%, 1%, 1.5% and 3%). The absorbance values (at 655nm) were determined using a microplate reader (Model 680, Bio-Rad). A standard curve was calculated and the samples' protein concentrations inferred.

Co-Immunoprecipitation (Co-IP)

One of the most used and rigorous demonstration of protein–protein interaction is the Co-Immunoprecipitation (Co-IP) of suspected complexes from cell extracts. Co-IP confirms interactions from a whole cell extract where proteins in their native conformation are present in a complex mixture of cellular components that may be required for successful interactions.

For Co-IP, 150µl of Protein G Sepharose 4 Fast Flow beads (GE Healthcare) were washed with Buffer C and centrifuged (14000rpm, 4°C) for three times, after which, 150µl of 1% BSA in Phosphate Buffer Saline (PBS) were added to the pellets.

Total protein lysate (750µg) was incubated with 1µg/µl MET clone 3D4 (Zymed) and as control the same amount of protein was incubated with 1µg/µl Normal Mouse IgG (Upstate Millipore). Mixtures were incubated at 4°C for 16 hours.

To each mixture, 50µl of the beads were added and a 45 minutes incubation at 4°C was performed, thus enabling the immobilization of the protein-protein complexes on the protein G sepharose beads. Unbound proteins were then removed by a series of washes in Buffer C. The protein complexes kept in the pellet were then eluted from the beads, dissociated and denatured by incubating with a solution of Laemmli 1.5%, bromophenol blue 0.25% and β-mercaptoethanol at 95°C for 5 minutes. SDS-PAGE of samples was then performed followed by Western blotting with specific antibodies for the bait (MET) and prey partners.

Small interfering RNA (siRNA) for MET downregulation

Short small interfering RNA (siRNA) is a class of short double-stranded RNA molecules (20-25 nucleotides), and interfering RNA (RNAi) is the methodology used to downregulate the expression of specific genes. In this specific case, *MET* was downregulated and its effects in other known proteins in the cells were assessed.

TPC-1, MDA-MB-231 and SkBr3 cells were plated in a 6-well tissue culture plate (TPP, Techno Plastic Products), 1.0×10^5 cells/well and 1.2×10^5 cells/well respectively, and grown in standard culture conditions until 60% confluence was reached. The respective culture medium was then changed to regular medium without antibiotics two hours before transfection. Cells were transfected with *MET*-specific siRNA oligonucleotides (Qiagen) and as control with Allstars Negative Control siRNA oligonucleotides (Qiagen) using LipoGen (Invivogen) following the manufacturer's instructions. The final concentration of siRNA was 100nM. After an incubation of 10 hours, the medium was replaced with regular medium. MET downregulation in transfected cells was confirmed by Western blot analysis 48h after.

SDS-PAGE and Western Blotting analysis

These methods are used to identify and quantify one or more specific proteins in a complex mixture sample.

SDS-PAGE – Sodium Dodecyl Sulfate – Poliacrylamide Gel Electrophoreses

The protein extracts were mixed with sodium dodecyl sulfate (SDS) and denaturated by heating at 65°C for 5 minutes.

Proteins were fractioned on 7.5% polyacrylamide gel prepared with 29:1 acrylamide/bis-acrylamide .

As marker Precision Plus Protein Standards – Dual Color (BioRad) was used.

Gels were run on BioRad mini-gel apparatus, at 50V for about 1hour and then at 100-150V for about 2 hours, until the front of the migration reached the bottom of the gel.

Electrophoresis buffer used was 1x Tris/Glycine/SDS Buffer (BioRad).

Western Blotting

After electrophoresis proteins were electroblotted onto nitrocellulose membranes (Hybond ECL, Amershan Life Science).

To transfer the proteins we used an electric current to pull them from the gel into the membrane, while the initial protein organization is maintained.

To visualize the uniformity, the overall effectiveness of the transferring and to locate molecular weight markers of the proteins, the membrane was stained with Ponceau S dye (SIGMA). The membrane was dried and then fragmented according to the protein MW's for the appliance of different primary antibodies.

The blocking step is crucial to prevent background signals resulting from nonspecific binding to the membranes. Blocking was performed using 5% non-fat dried milk in PBS with 0.5% Tween20. The incubation was done at room temperature (RT) for 1hour with agitation.

The primary antibodies were diluted in 5% non-fat dried milk in PBS 0.5% Tween20 according to the dilutions shown in the table 1, with the exception of pErk1/2 that was diluted in 5% BSA in PBS with 0.5% Tween20.

Table 1. Primary antibodies and respective incubation conditions used for WB analysis.

Target	Antibody	WB conditions
ErbB-2	ErbB-2, clone N3/D10, mouse monoclonal Ref. CBL755, Chemicon	1:1000, 1h, RT
MET	MET, clone 3D4, mouse monoclonal Ref. 18-7366, Zymed	1:1000, 1h, RT
EGFR	EGFR, rabbit polyclonal Ref. #2232, Cell Signaling	1:1000, 1h, RT
pErk 1/2	p44/42MAPK (Thr202/Tyr204) mouse monoclonal Ref. 9106, Cell Signaling	1:1000, 1h, RT
Erk 1/2	p42/p44MAPK rabbit polyclonal Ref. 9106, Cell Signaling	1:1000, 1h, RT
Actin	Actin, clone I-19, goat polyclonal Ref. sc-1616, Santa Cruz Biotechnology	1:2000, 1h, RT

Incubation with the primary antibody was performed for 1h at RT. After the primary antibodies incubation, the membranes were washed in PBS with 0.5% Tween-20 for five times, 5 minutes each.

The appropriate secondary antibodies conjugated with horseradish peroxidase (HRP) (Santa Cruz Biotechnology) were then used in a 1:2000 dilution in 5% non-fat dried milk in PBS with 0.5% Tween20 to perform a 1 hour incubation with agitation (RT).

After the secondary antibodies incubation the membranes were washed in PBS with 0.5% Tween-20 for 5 times, 5minutes each.

The membranes were developed with enhanced chemiluminescent (ECL) reagent (Amersham Life System Science), according to the manufacturer's instructions. The peroxide buffer reacts with the HRP to emit light and the luminol/enhacer solution intensifies the signal obtained. The signals were detected by exposing the membranes to X-ray film (Kodak) for a suitable period of time.

Immunofluorescence

Immunofluorescence is a technique used for the labeling of proteins with fluorescent dyes. This method can be divided in three steps: cell culture, fixation and cell staining.

In the cell culture, the cells to be stained are attached to a solid support to allow the easy handling in the other steps. To achieve this, the cells were grown in coverslips and fixed at semi-confluence.

The step of fixation and permeabilization of the cells ensures free access of the antibody to its antigen. The fixation was done using 4% paraformaldehyde in PBS (MERCK). Paraformaldehyde is a cross-linking reagent that forms intermolecular bridges, normally through free amino groups, creating a network of linked antigens that preserves the cell structure. After fixation, cells were permeabilized with 0.2% Triton X-100 in PBS (Applichem). This step is needed to the fully access of the antibody to the antigen.

The cell staining step involves the blocking step, the incubation with the primary antibody and the incubation with secondary antibody labeled with a fluorochrome.

Cells were blocked for 30 minutes with 5% BSA in PBS solution under agitation (the BSA has the same function as the non-fat dried milk from the blocking step of the Western Blotting).

Incubations with the primary antibodies were performed for 16 hours at 4°C with specific antibody dilutions in UltraAb Diluent (Lab Vision Corporation) (Table 2).

Table 2. Primary antibodies and respective incubation conditions used for Immunofluorescence analysis.

Target	Antibody	Abs conditions
ErbB-2	ErbB-2, clone N3/D10, mouse monoclonal Ref. CBL755, Chemicon	1:60, 16h, 4°C
MET	MET, clone 3D4, mouse monoclonal Ref. 18-7366, Zymed	1:100, 16h, 4°C
EGFR	EGFR, rabbit polyclonal Ref. #2232, Cell Signaling	1:250, 16h, 4°C

After the primary antibodies incubation the cells were washed in PBS 3 times for 5 minutes each.

The cells were then incubated with the appropriated secondary antibodies conjugated with fluorescein isothiocyanate (FITC) (DakoCytomation) for 45 minutes at room temperature, protected from the light.

After the incubation the cells were washed with PBS three times 5 minutes each.

The coverslips were inverted onto glass slides in mounting medium with DAPI (Vectashield) and seen under the microscope.

The nuclei and specific signals obtained were analysed with a fluorescence microscope (Axio Imager Microscope Zeiss), the nuclei stained with DAPI were detected in UV light as blue fluorescence, (filter 49, excitation 358nm, emission 463nm), and the signals were detected in blue light as green fluorescence (filter 38 HE, excitation 470/40nm, emission 525/50nm).

Proximity Ligation Assay

An important part of the work developed was the establishment and optimization of the recent technique Proximity Ligation Assay (PLA). PLA is a new technology developed in the Department of Genetics and Pathology at the University of Uppsala, Sweden, by Ulf Landegren and colleagues. It is a protein detection method that combines dual recognition of target proteins by pairs of affinity probes generating an amplifiable DNA reporter molecule which acts as a surrogate marker for the detected protein or interacting proteins.

The PLA enables the microscopic detection and visualization of individual proteins, protein modifications and protein complexes in tissues and cell samples.

The assay is based on different techniques that are put together to yield high sensitivity. A pair of probes with attached oligonucleotides is brought into close proximity by binding adjacent proteins and serves as templates for the circularization of so-called connector oligonucleotides by enzymatic ligation. The circularized DNA strands remain hybridized to the proximity probes, upon addition of phi29 DNA polymerase, and one of the oligonucleotides serves as a primer for the rolling circle amplification (RCA), in the process unwinding the other oligonucleotide from the DNA circle. The amplification reaction generates a randomly coiled, single-stranded product composed up to 1000 complements of DNA circle, covalently linked to an antibody-antigen complex. This product is easily detected through hybridization of complementary fluorescence-labelled oligonucleotides as showed in Figure 6 (Soderberg *et al.*, 2006).



Figure 6. Schematic presentation of Proximity Ligation Assay method adapted from Duolink PLA User Manual.

The samples used were both thyroid and breast cell lines, grown in coverslips, fixed with 4% paraformaldehyde in PBS (MERCK) and permeabilized with 0.2% Triton X-100 in PBS (Appllichem).

The protocol can be divided in seven steps: blocking, primary antibodies incubation, PLA probes, hybridization, ligation, amplification and detection. The solutions are from “Duolink 100 in situ PLA anti rabbit anti mouse kit” (OLINK).

All the stock solutions prior being used were diluted 1:5 in high purified water.

The blocking solution was added to the coverslips and incubated the in a pre-heated humid chamber for 30 minutes at 37°C.

The primary antibodies were incubated according to the Table 3, following the manufacturer’s instructions for the combination of the antibodies. The negative control had no primary antibodies, being the coverslip covered only with Antibody Diluent. The Blocking Solution was removed from the coverslips and the primary antibody solution was added to each sample and incubated in a humid chamber for 16h at 4°C.

Table 3. Primary antibodies for the interactions used for Proximity Ligation Assay.

Interaction Target	Antibodies	Abs conditions
ErbB-2 – ErbB-2	<ul style="list-style-type: none"> ErbB-2 clone N3/D10, mouse monoclonal Ref. CBL755, Chemicon ErbB-2 rabbit polyclonal Ref. A0485, Dako Cytomation 	<ul style="list-style-type: none"> 1:40 1:100
MET – MET	<ul style="list-style-type: none"> MET clone 3D4, mouse monoclonal Ref. 18-7366, Zymed MET clone CVD13, rabbit polyclonal Ref. 18-2257, Zymed 	<ul style="list-style-type: none"> 1:100 1:200
ErbB-2 – MET	<ul style="list-style-type: none"> ErbB-2 clone N3/D10, mouse monoclonal Ref. CBL755, Chemicon MET clone CVD13, rabbit polyclonal Ref. 18-2257, Zymed 	<ul style="list-style-type: none"> 1:40 1:200
MET - EGFR	<ul style="list-style-type: none"> MET clone 3D4, mouse monoclonal Ref. 18-7366, Zymed EGFR, rabbit polyclonal Ref. #2232, Cell Signaling 	<ul style="list-style-type: none"> 1:100 1:250
ErbB-2 – EGFR	<ul style="list-style-type: none"> ErbB-2 clone N3/D10, mouse monoclonal Ref. CBL755, Chemicon EGFR, rabbit polyclonal Ref. #2232, Cell Signaling 	<ul style="list-style-type: none"> 1:40 1:250

After the incubation the coverslips were washed with Tris-Buffered Saline – Tween 20 (TPS-T) for 2 times, 5 minutes each, under gentle agitation

Then two PLA probes were diluted 1:5 in Antibody Diluent, added to the coverslips and incubated in a pre-heated humid chamber for a maximum of 2h at 37°C.

The coverslips were washed in TBS-T for 2 times, 5 minutes each, and the Hybridization solution was added to each sample and incubated in pre-heated humidity chamber for 15 min at 37°C.

The coverslips were washed with TBS-T for 1 minute under gentle agitation, the Duolink Ligase was diluted 1:40 to the Ligation solution and the coverslips were incubated in a pre-heated humid chamber for 15 minutes at 37°C. After the incubation the coverslips were washed with TBS-T for 2 times, 5 minutes each.

The Duolink Polymerase was added to the Amplification solution at 1:80 dilution and the samples were incubated in a pre-heated humid chamber for 90 minutes at 37°C. The coverslips were washed with TBS-T for 2 times 5 minutes each.

The Duolink Detection was added to each sample and incubated in a pre-heated humid chamber for 60 minutes at 37°C protected from the light.

The coverslips were washed in a series of washes, 2 minutes each, in SSC 2x, SSC 1x, SSC 0.2x, SSC 0.02x, and then 20 seconds in 70% ethanol. The coverslips were protected from light during the procedure.

For the preparation of the imaging slides were covered with 3µl of mounting medium (Vectashield) and the dried coverslip were place on it.

The nuclei and signals obtained were analysed with a fluorescence microscope (Axio Imager Microscope Zeiss), the nuclei were stained with Hoechst 33342 and detected in UV light as blue fluorescence, (filter 49, excitation 346nm, emission 460 nm), and the signals were detected in green light as red fluorescence (filter 43 HE, excitation 550/25nm, emission 605/70nm).

The images captured on the fluorescent microscope were analysed with “BlobFinder” software, developed in the Centre for Image Analysis at Uppsala University, which counts the hybridization signals in each cell.

Immunohistochemistry

The immunohistochemistry technique enables the localization of proteins in cells of a tissue section exploiting the well-known principle of antibody-antigen specific binding.

The immunohistochemistry performed was based on a streptavidin-biotin staining method where a biotinylated secondary antibody links the primary antibodies to a streptavidin-peroxidase conjugate. A single primary antibody was therefore, associated with multiple peroxidase molecules that considerably increased its sensitivity. Peroxidase activity in the presence of the electron donor resulted in the formation of an enzyme-substrate complex, which oxidized the electron donor 3,3'-diaminobenzidinetetrahydrochloride (DAB) producing a brown end product highly insoluble in organic solvents.

Immunohistochemical procedure were performed in the TMAs using the primary antibody towards MET, clone CVD13 rabbit polyclonal (Zymed). The negative control used was a thyroid preparation known positive for MET protein.

The TMAs and the negative control were deparaffinised in Clear-Rite (Richard-Allan Scientific, Thermo Scientific) for 20 minutes and rehydrated in graded alcohols (100% and 70% v/v), and ddH₂O 5 minutes each. The antigen retrieval used was the Target Retrieval Solution pH 9.0 (DakoCytomation) for 20 minutes at 98°C in a water bath.

After being at RT for at least 20 minutes, the preparations were then washed in PBS 0.02% Tween-20 for 3 times, 5 minutes each, and incubated with 200µL of 3% v/v hydrogen peroxide in methanol for 10 minutes at room temperature, to inhibit endogenous peroxidase. In order to block unspecific binding, an incubation of 10 minutes at room temperature was performed using 100µL Ultra V Block solution (Lab Vision Corporation). Sections were then incubated, overnight at 4°C, with the primary antibody previously diluted 1:400 in UltraAb Diluent (Lab Vision Corporation), and the negative control was incubated only with UltraAb Diluent.

The next day the samples were washed 3 times, 5 minutes each, in PBS 0.02% Tween-20 and overlaid with 100µL of secondary antibody (Biotinylated Goat Anti-Polyvalent, Lab Vision Corporation) for 10 minutes.

Localization was performed via the application of 100µL of Streptavidin Peroxidase (Lab Vision Corporation) for 10 minutes at room temperature. The sections were then stained with 100µL of liquid (DAB) (DakoCytomation Liquid DAB + Substrate Chromogen System, DAKO Corporation) for 5 minutes and counterstained with Meyer's Haematoxylin (J. T. Baker, Deventer, Holland) during 2 minutes.

Using graded alcohols, 95% and 100%, sections were dehydrated for 5 minutes in each and placed in Clear-Rite to allow further coverslips mounting with Entellan (Richard-Allan Scientific).

The stained TMAs were further visualised, and analysed in a multi-head microscope (Zeiss Axioskop2) and a proper classification was performed by two observers, being one a specialized Pathologist. The MET expression was assessed in terms of intensity and extension of the staining on the cellular location according to the table 4. Only a clear membranar staining was considered as specific. Cases with MET intensity of staining 0 or 1+ were considered negative expression, and cases with 2+ and 3+ were considered positive expression.

Table 4. Immunohistochemical classification.

Score	Intensity of staining
0	Absence of staining
1+	Weak staining
2+	Intermediate staining
3+	Strong staining

Statistical analysis

The analysis of the immunohistochemistry results was completed using SPSS Statistics 17.0 for Windows software. Correlations between clinicopathological factors and MET were performed using Pearson chi-square test. The survival of the patients was performed by obtaining the Kaplan Meier survival curve, with significance evaluated using Log-rank test.

The prognostic significance was assessed using Univariate Cox-proportional hazards model, and the determination of independent prognostic factors on the survival was performed by Multivariate analysis applying Cox regression model on the variables with statistical significance in univariate analysis. The cases with a follow-up minor than 2 years were not taken in account. *P* value was considered significant when $P < 0.05$.

Results

Expression of MET, ErbB-2 and EGFR in carcinoma-derived cell lines

MET, ErbB-2 and EGFR are coexpressed in thyroid and breast carcinomas cell lines.

A preliminary classification and quantification of the expression of the proteins MET, ErbB2 and EGFR in the different cell lines was made by Western blot and Immunofluorescence.

From all the cell lines, four that expressed all the target RTKs were selected, TPC-1 and 8505C from papillary and undifferentiated thyroid carcinomas, respectively, and MDA-MB-231 and SkBr3 from basal and ErbB-2 OE breast carcinomas, respectively. The selected cell lines allowed a good coverage of different subtypes of carcinomas and the respective characterization in the subsequent studies.

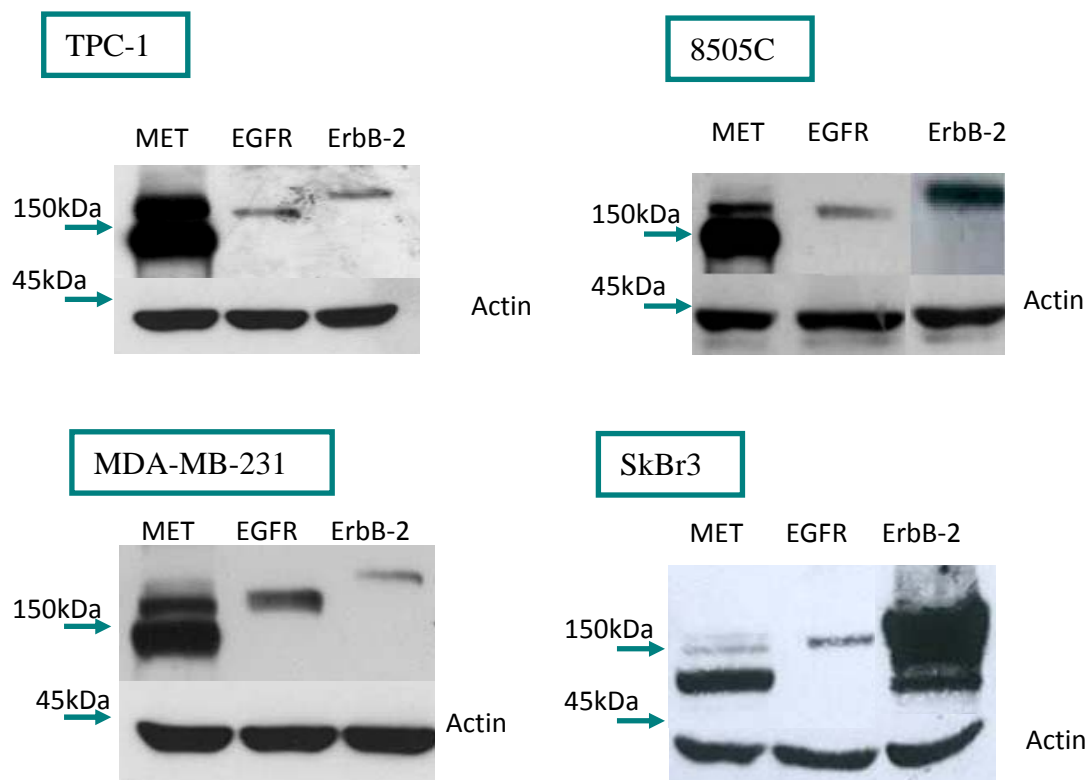


Figure 7. MET (145kDa), EGFR (170kDa) and ErbB-2 (185kDa) are present in both thyroid (TPC-1 and 8505C) and breast (MDA-MB-231 and SkBr3) cell lines. Whole cell lysates from TPC-1, 8505C, MDA-MB-231 and SkBr3 were separated by SDS-PAGE and analysed for MET, EGFR and ErbB-2 expression by Western Blot. Actin was used as loading control.

As shown by Western Blot (Figure 7) and Immunofluorescence (Figure 8) MET, EGFR and ErbB-2 are expressed, at different levels, in all the selected cell lines.

By immunofluorescence the target RTKs expression are observed mainly in the cytoplasm and in the membrane. The Western Blot and Immunofluorescence images from the remain cell lines are shown in the Annexe 2.

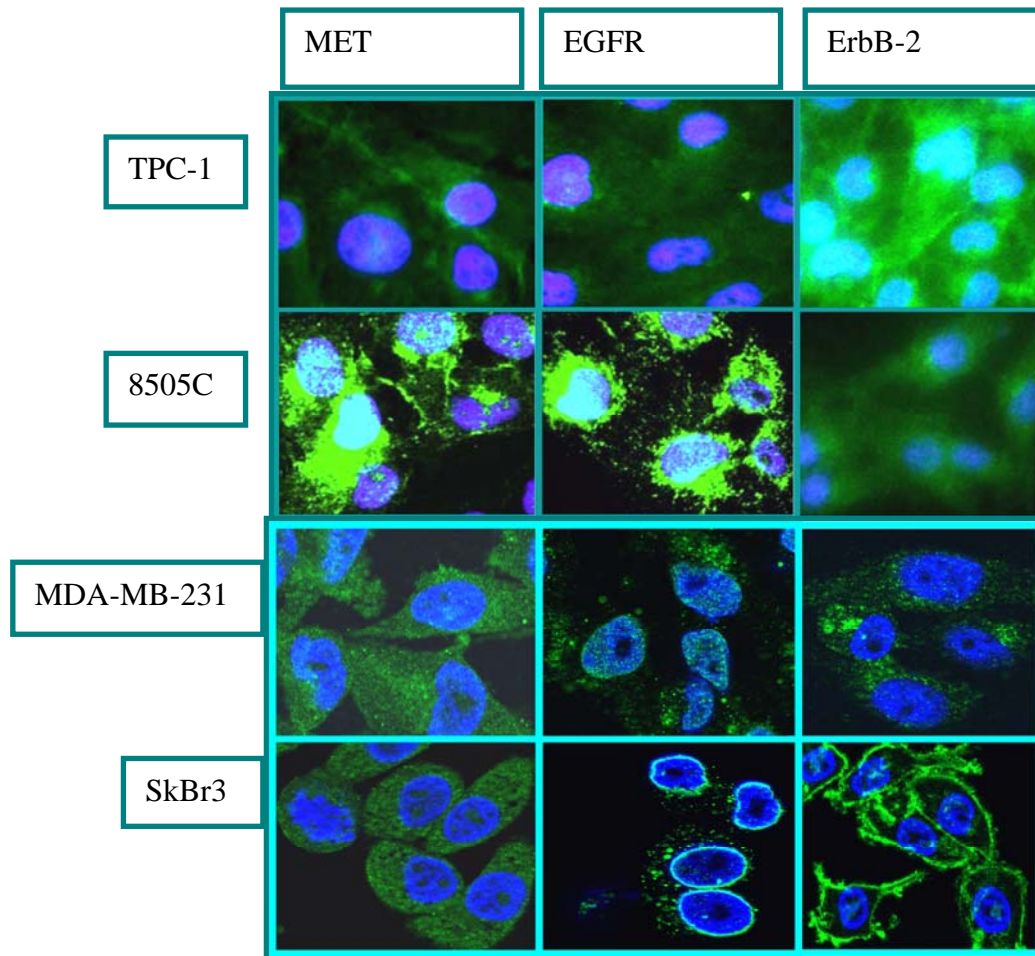


Figure 8. MET, EGFR and ErbB-2 are present in both thyroid (TPC-1 and 8505C) and breast (MDA-MB-231 and SkBr3) cell lines (400x). The MET, EGFR and ErbB-2 are stained green (FITC) and the nuclei are stained blue (DAPI).

MET, EGFR and ErbB-2 interactions.

The presence of RTKs interaction complexes were assessed by Co-Immunoprecipitation and by Proximity Ligation Assay.

ErbB-2 co-immunoprecipitated with MET but EGFR did not, in all the four cell lines in study. These results suggest that only ErbB-2 and MET are found in a protein complex and that EGFR does not form a physical complex with MET (Figure 9). The WB of MET is used as a control to demonstrate the endogenous levels of MET expression.

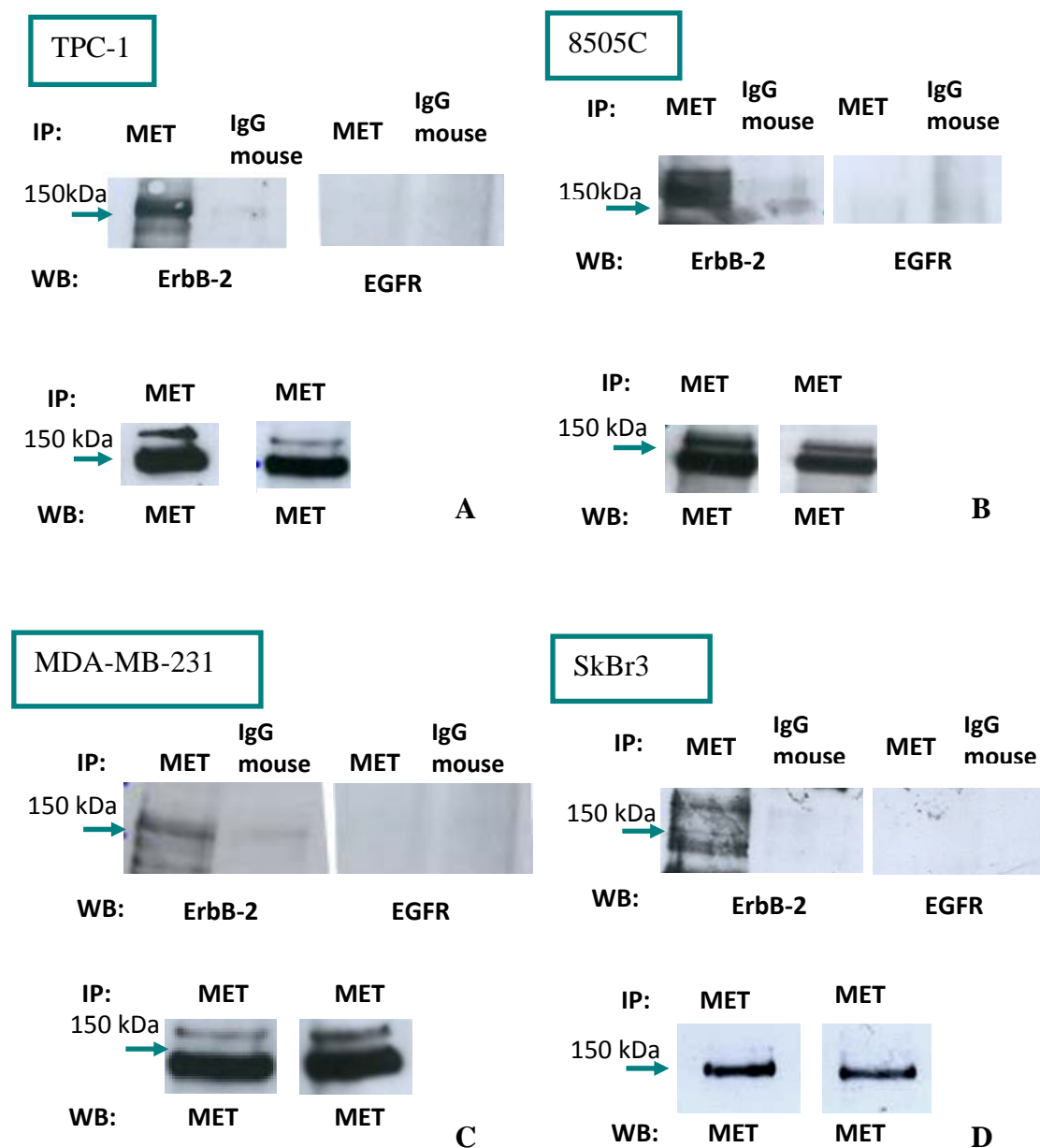


Figure 9. MET interacts with ErbB-2, but not with EGFR in TPC-1 (A), 8505C (B), MDA-MB-231(C) and SkBr3 (D). Immunoprecipitation with IgG mouse was used as a negative control in each experiment.

In the Proximity Ligation Assay the hybridization signals found in the cells represent the interaction between the proteins in study. A fluorescence microscope image overlapped with a schematic representation of the software analysis can be seen on figure 10.

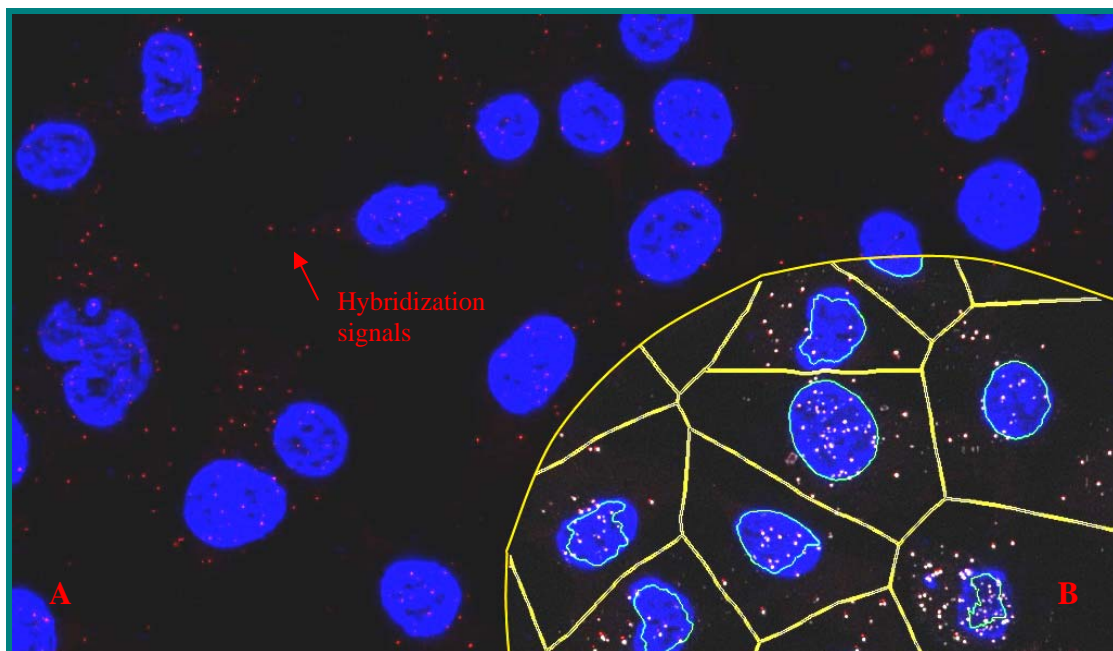


Figure 10. The MET- ErbB-2 interaction in the 8505C cell line by PLA technique is shown (as an example of PLA results). A – Fluorescence microscope image, the nuclei are stained in blue and the hybridization signals in red (400x). B (inset) – Overlay between images from the fluorescent microscope and the software analysis scheme.

For each cell line, the interactions between MET and ErbB-2 were characterized. In each interaction assay, negative control experiments were performed which resulted in negligible amounts of signals (Figure 11).

In all the cell lines the interaction found in higher number was MET–MET, with the exception of SkBr3 which due to the overexpression of ErbB-2 the ErbB-2–ErbB-2 was the principal interaction. The MET-ErbB-2 interaction was found in all the cell lines in study, confirming the previous Co-IP results.

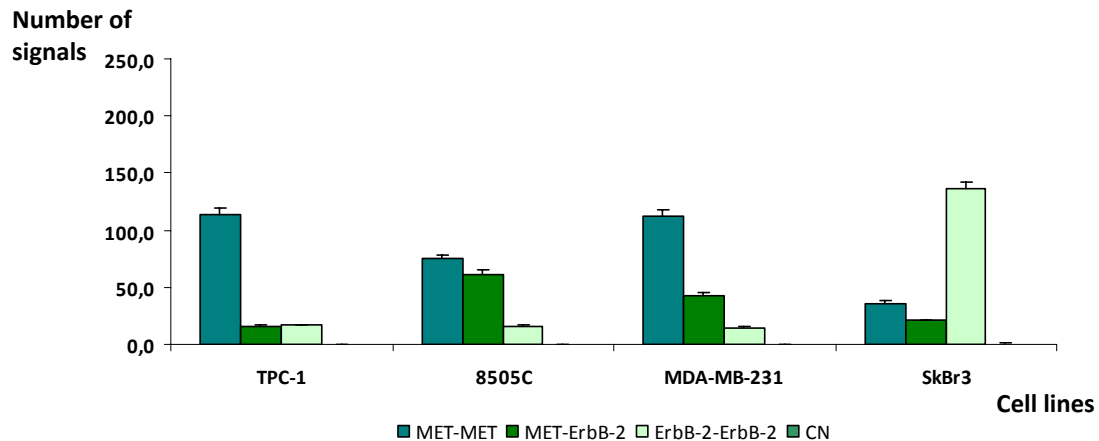


Figure 11. MET and ErbB-2 interactions in TPC-1, 8505C, MDA-MB-231 and SkBr3 cell lines, analysed by Proximity Ligation Assay. The histograms indicate the number of MET and ErbB-2 interactions (residual control values are not always visible). CN, negative control.

Increased level of ErbB-2 expression upon downregulation of MET.

The MET expression was downregulated by treatment of TPC-1, MDA-MB-231 and SkBr3 cells with MET siRNA. Under knockdown conditions western blot was performed to assess variations in the expression of MET, ErbB-2, phospho and total Erk and PLA was performed to assess the MET–MET, MET–ErbB-2 and ErbB-2–ErbB-2 interactions.

As shown in Figure 12, the downregulation of MET was concomitant with an increase of ErbB-2 expression in TPC-1 (1.3-fold increase) and MDA-MB-231 (1.5-fold increase) cells. The SkBr3 cells didn't show an evident increase of ErbB-2, however, in this cell line the number of ErbB-2 homodimers increase in comparison to the non-downregulated cells (Figure 13).

No differences were seen in phosphorylated or total ERK expression either in the control or MET siRNA conditions.

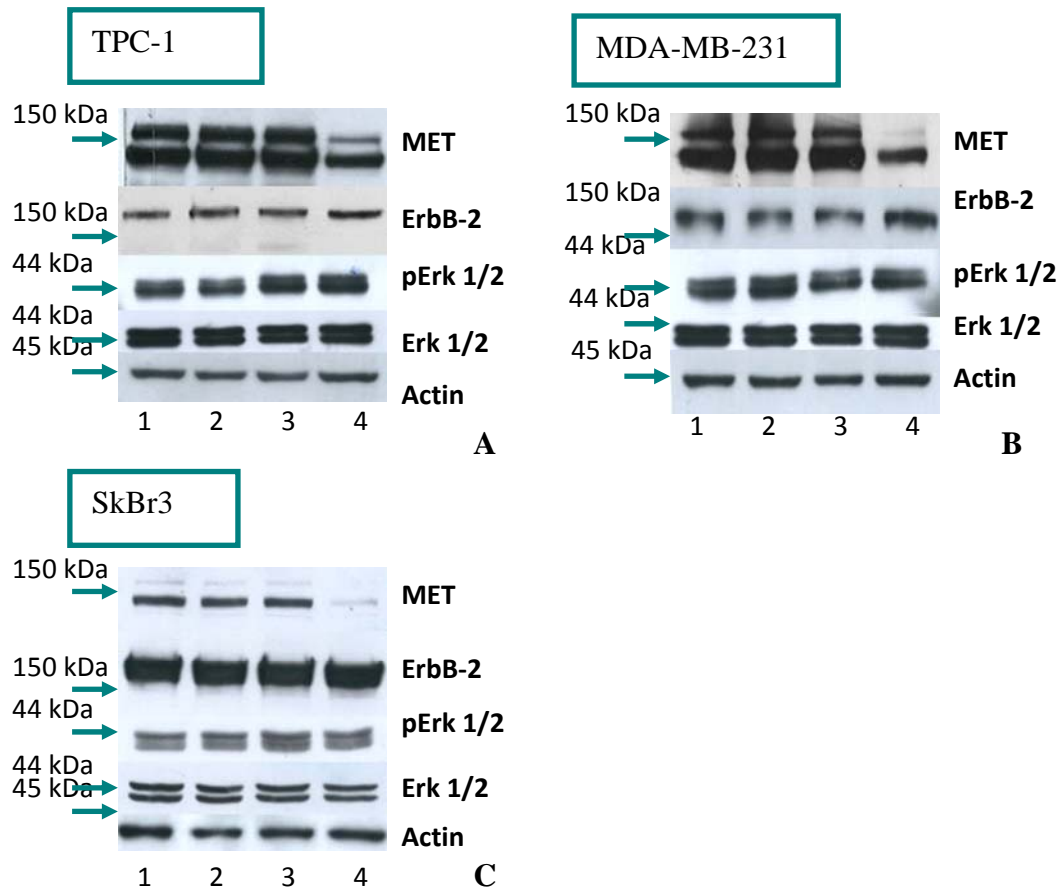


Figure 12. Western blot analysis of MET, ErbB-2, Erk1/2 activation in TPC-1 (A), MDA-MB-231 (B), and SkBr3 (C) cells after MET downregulation. Actin was used as control. 1. Control cells (no treatment); 2. Control cells treated only with Lipogen; 3. Control cells treated with scramble RNA oligonucleotides; 4. Cells treated with MET siRNA.

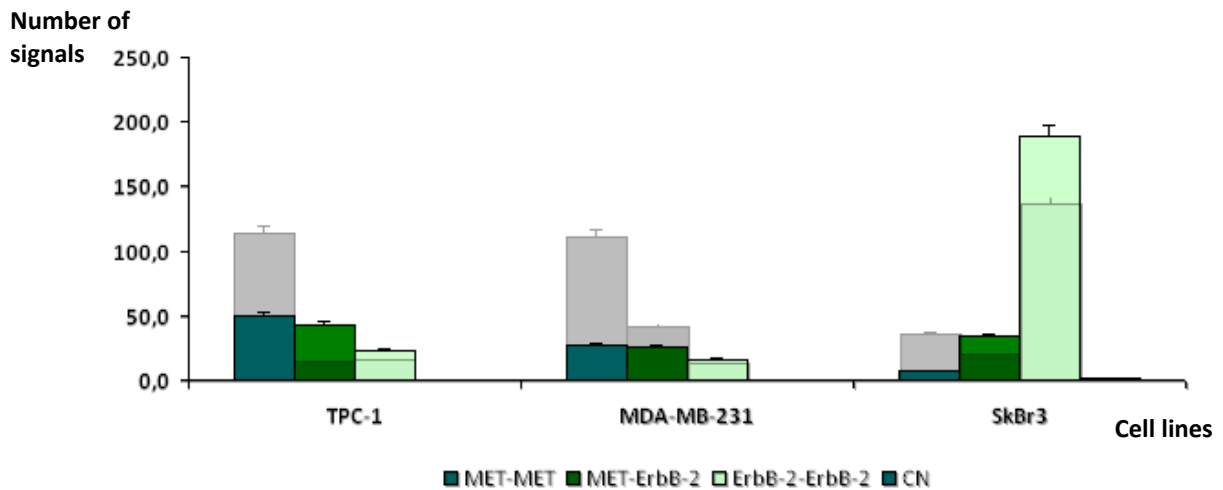


Figure 13. MET and ErbB-2 interactions analysed by Proximity Ligation Assay in TPC-1, MDA-MB-231 and SkBr3 cell lines after MET downregulation. The histograms indicate the number of MET and ErbB-2 interactions (negative control residual values not always visible). The dark shade histograms demonstrate the MET and ErbB-2 interactions in the cell lines without MET downregulation. CN, negative control.

In all the cell lines in study the MET downregulation is quite evident by PLA analysis (Figure 13). Also a slightly increase in the number of MET-ErbB-2 and ErbB-2-ErbB-2 dimers is seen in TPC-1 and SkBr3.

MET in Tissue Samples

Immunostaining for MET

The breast tumours used in this part of the study had been previously classified in subtypes and by grade. In the series used the most established markers for breast carcinogenesis (ER, PR, ErbB-2, P53, P63 and P-cadherin) had already been tested.

MET staining was localised both in cytoplasm and membrane (Figure 14), but only the membrane staining was taken in account, being the cytoplasm staining considered “background” of the primary antibody. The MET staining exhibited considerable variations between the different types of tumours, but was substantially stronger than in the surrounding normal tissues where almost no staining was observed.

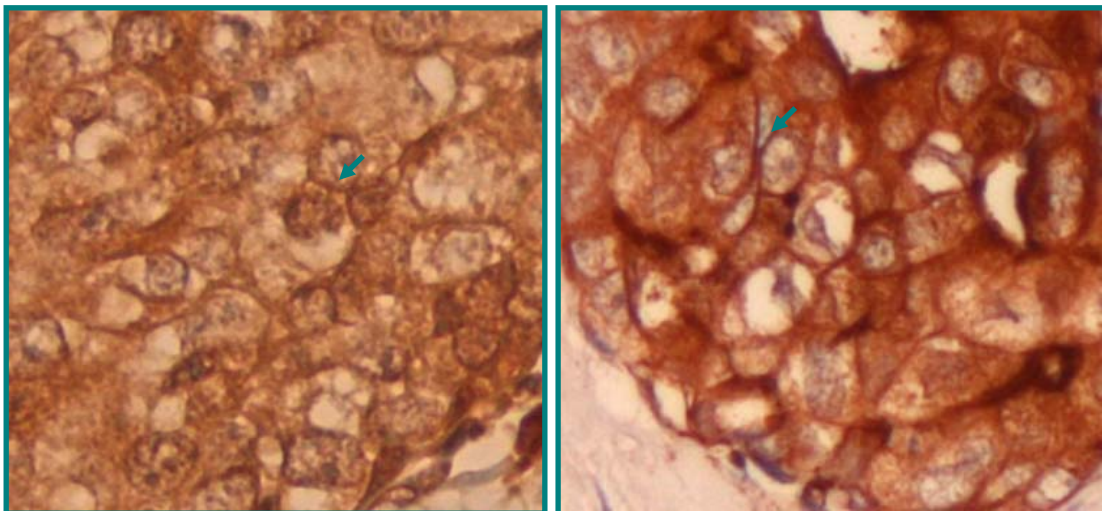


Figure 14. Immunohistochemical staining of MET in two different breast cancer cases (400x). MET membranar expression considered as positive staining is indicated by blue arrows.

The Pearson chi-square analysis results are summarized in Table 5. MET membranar staining was correlated with the molecular subtypes classification ($P=0.002$), ErbB-2

expression ($P=0.038$), and absence of ER ($P=0.004$). Also a significant correlation between MET and Grade ($P=0.023$) was observed.

MET expression was not significantly correlated to other establish prognostic factors such as age, lymph node metastasis, PR, P-cadherin, EGFR, p53 and p63.

Table 5. Statistical comparison between the presence/absence of MET and the clinicopathologic characteristics of breast cancer.

Variables		N	MET N(%)		P value ^a
			+	-	
Molecular subtypes	Luminal	124	43 (34.68%)	81 (65.32%)	0.002
	ErbB-2 OE	20	15 (75.00%)	5 (25.00%)	
	TN	51	25 (49.02%)	26 (50.98%)	
ErbB-2	+	32	19 (59.38%)	13 (40.62%)	0.038
	-	167	66 (39.52%)	101 (60.48%)	
ER	+	121	42 (34.71%)	79 (65.29%)	0.004
	-	78	43 (55.13%)	35 (44.87%)	
PR	+	80	31 (38.75%)	49 (61.25%)	0.354
	-	119	54 (45.38%)	65 (54.62%)	
EGFR	+	13	8 (61.54%)	5 (38.46%)	0.156
	-	186	77 (41.40%)	109 (58.60%)	
p63	+	3	1 (33.33%)	2 (66.67%)	0.741
	-	196	84 (42.86%)	112 (57.14%)	
p53	+	43	20 (46.51%)	23 (53.49%)	0.570
	-	156	65 (41.67%)	91 (58.33%)	
P-cadherin	+	53	27 (50.94%)	26 (49.06%)	0.157
	-	146	58 (39.72%)	88 (60.27%)	
Lymph node metastasis	+	87	42 (48.28%)	45 (51.72%)	0.183
	-	74	28 (37.84%)	46 (62.16%)	
Grade	I	90	32 (35.56%)	58 (64.44%)	0.023
	II	79	34 (43.04%)	45 (56.96%)	
	III	24	16 (66.66%)	8 (33.34%)	
Age		199	85 (42.71%)	114 (57.29%)	0.611

a. P value (Pearson chi-square test) was considered significant when $P<0.05$. Statistically significant observations are in blue-boldface.

To evaluate the prognostic significance of MET in the invasive breast cancer disease a Kaplan-Meier survival analysis was performed (Figure 15). The Kaplan-Meier curve

demonstrated that MET expression was related to a worse prognosis having these patients a short disease-related survival in the 13-year follow-up period ($P=0.004$).

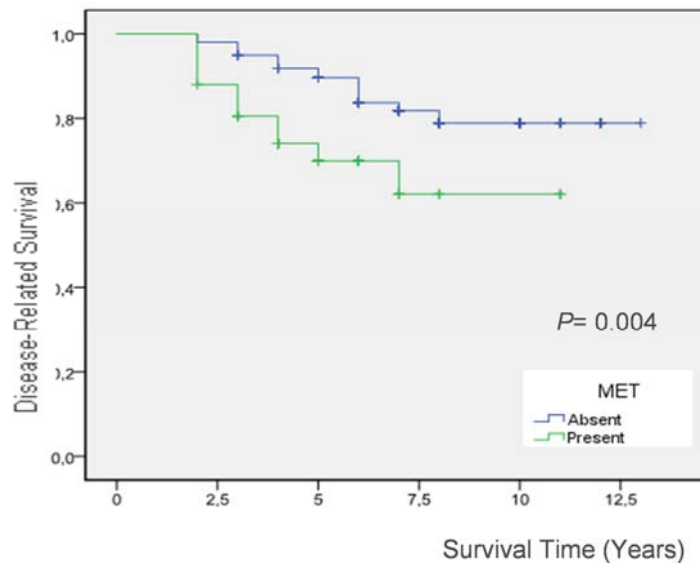


Figure 15. Kaplan-Meier analysis of disease-related survival demonstrates that the presence of MET tend to increase a worse prognosis and an earlier death. Statistical significance was assessed using the Log-rank test.

In Luminal, ErbB-2 OE and triple negative subtypes the Kaplan Meier test was also performed to observe the role of MET in the disease-related survival of each subtype of tumours (Figure 16).

In the patients with luminal subtype tumours the Kaplan-Meier curve is identical to that obtained for the overall subtypes being MET expression correlated with a shorter disease-related survival ($P=0.015$). The same tendency found in the patients with Luminal subtype was observed those with triple negative tumours, although without reaching significance. At variance the patients with ErbB-2 OE tumours expressing MET presented a better outcome, showing a tendency to higher disease-related survival.

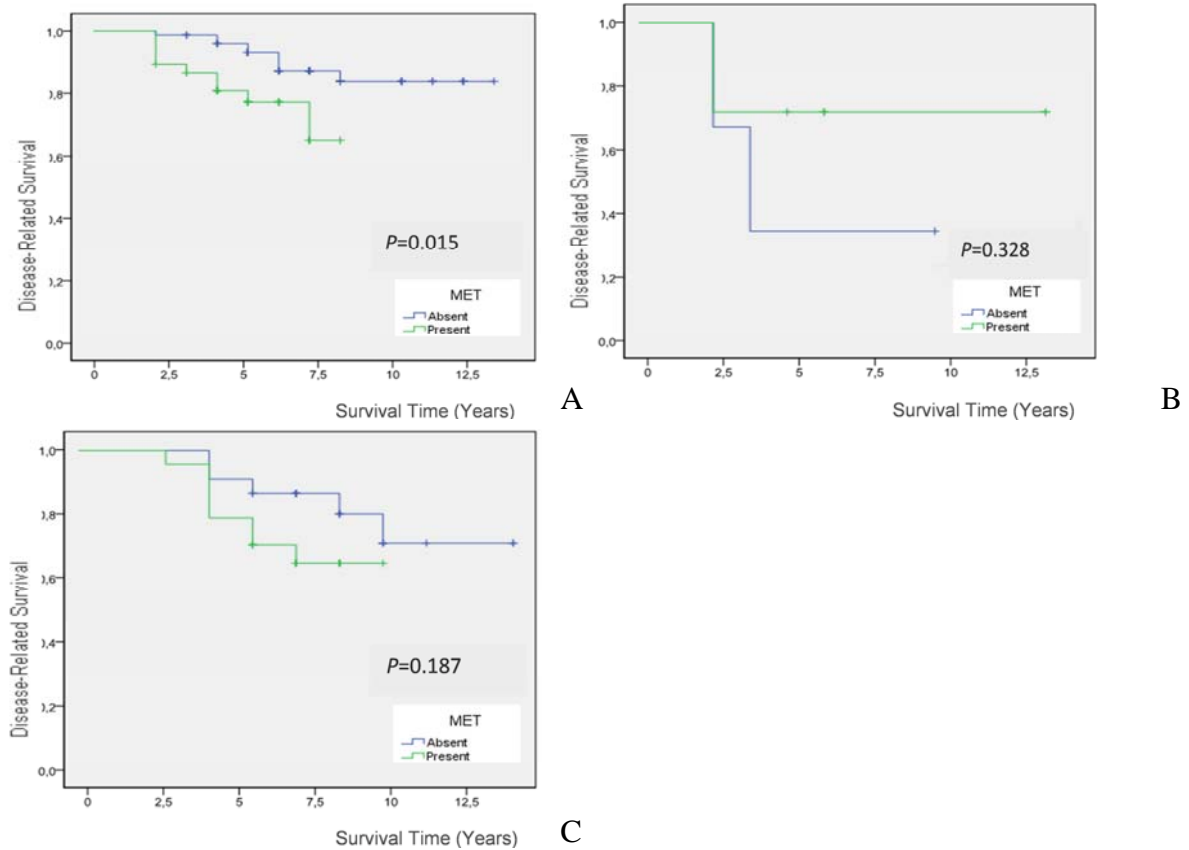


Figure 16. Kaplan-Meier analysis of disease-related survival in Luminal (A), ErbB-2 OE (B) and Triple negative (C) subtypes of tumours. Statistical significance was assessed using the Log-rank test.

Clinicopathological factors and survival.

To determine the predictive influence on survival of breast cancer prognostic variables a univariate analysis of 11 clinicopathological factors was performed. The prognosis was significantly related to 8 of the 11 variables analysed, MET, ErbB-2, ER, PR, p63, P-cadherin, grade and age (Table 6), where ER and PR had a correlation with better prognosis (Relative risk <1) and the remain factors were correlated with a worse prognosis (Relative risk >1).

Table 6. Univariate analysis of the clinicopathologic factors for the 13-year disease-related survival.

Variables	Univariate Analysis		
	Relative Risk	<i>P</i> value _a	95% C.I.
MET	2.554	0.006	1.303 - 4.996
ErbB-2	2.320	0.025	1.111 - 4.842
ER	0.493	0.021	0.271 - 0.898
PR	0.509	0.047	0.261 - 0.991
EGFR	1.643	0.408	0.507 - 5.321
p63	4.482	0.040	1.075 - 18.693
p53	1.864	0.057	0.981 - 3.541
P-cadherin	2.006	0.030	1.071 - 3.757
Subtypes	1.371	0.051	0.998 - 1.882
Grade	1.883	0.002	1.273 - 2.785
Age	1.026	0.033	1.002 - 1.050

a. *P* value was considered significant when $P < 0.05$ by Cox-proportional hazards model. C.I. confidence interval. Statistically significant observations are in blue-boldface.

Multivariate analysis using the Cox proportional hazards model involving the 8 significant factors determined by Univariate analysis was performed (Table 7).

MET was the only clinicopathological factor that remains significant ($P=0.041$) in this analysis, which indicates that MET is an independent predictor of poor prognosis, confirming the previous data.

Table 7. Multivariate analysis of the 13-year disease-related survival using only the statistically significant clinicopathologic factors from the univariate analysis.

Variables	Multivariate Analysis		
	Relative Risk	<i>P</i> value _a	95.0% C.I.
MET	2.115	0.041	1.030 - 4.345
ErbB-2	1.955	0.135	0.812 - 4.704
ER	1.067	0.889	0.430 - 2.651
PR	0.683	0.454	0.251 - 1.856
p63	3.741	0.226	0.442 - 31.689
P_cadherin	1.382	0.440	0.608 - 3.139
Grade	1.366	0.225	0.826 - 2.259
Age	1.027	0.074	0.997 - 1.058

a. *P* value was considered significant when $P < 0.05$ by Cox-proportional hazards model. C.I., confidence interval. Statistically significant observations are in blue-boldface.

Discussion

Historically, RTKs define the prototypical class of oncogenes involved in most forms of human malignancies (Robinson *et al.*, 2000).

This study is focused on RTKs expression and interactions of ErbB and HGFR families that have overlapping functions in initiation and progression of cancer. EGFR and ErbB-2 are implicated in promoting proliferation and survival and MET has an important role in cell motility and epithelial/mesenchymal transition, although its function is a matter of continuous debate (Agarwal *et al.*, 2009).

This work was primarily performed in five thyroid carcinoma-derived cell lines (TPC-1, 8505C, C643, K1 and XTC-1). The MET, EGFR and ErbB-2 expression was detected, in different levels, by Western Blot and Immunofluorescence and their interactions were analysed by Proximity Ligation Assay and Co-Immunoprecipitation. Subsequently the MET–ErbB-2 interaction was the only dimer confirmed between ErbB and HGFR families. In 2007 Guo *et al.*, to understand the sensitivity of some tumours to target kinase inhibitors, described the physical interaction MET-EGFR and observed that Gefitinib, a selective inhibitor towards EGFR, besides inhibiting EGFR also inhibited phosphorylation of ErbB-2, ErbB-3 and MET in NSCLC cell lines. They also predicted that MET could interact with others RTKs like EGFR, ErbB-2 and ErbB-3 in MKN45, a gastric carcinoma-derived cell line.

In 2008 Shattuck *et al.*, described that MET and ErbB-2 are co-expressed in ErbB-2 OE breast cancer cells and tumours. When they treated the cell lines with Trastuzumab, a humanized monoclonal antibody directed against ErbB-2, they observed a significant increase in MET expression, accompanied by an increase in MET transcript levels, which they observed that contributed to Trastuzumab resistance through the sustained activation of downstream signalling activation.

In 2009 Agarwal *et al.*, described that MET physical interacts with both EGFR and ErbB-2 in NSCLC cell lines with overexpression/ overactivation of MET. In this study they suggested a simultaneous inhibition of multiple RTKs to effectively abrogate tumour cell growth.

Since our results were consistent with the recent studies from Guo *et al.*, 2007; Shattuck *et al.*, 2008 and Agarwal *et al.*, 2009, with the exception that we did not observed MET-EGFR interaction, in collaboration with the Breast Cancer Group, aiming a better understanding of the clinical and prognostic significance of the MET–ErbB-2 interaction, we decided to extend our work to breast cancer.

The breast cancer is a very well studied cancer model. It is a very aggressive disease, where ErbB-2 is a well studied and important prognosis factor with already a targeted therapy approved, Trastuzumab. Due to these facts we have decided that breast cancer should be our model to better understand the impact of MET expression and interactions with ErbB-2.

The selected breast carcinoma-derived cell lines used were SkBr3, from ErbB-2 OE tumour subtype, and MDA-MB-231, from basal tumour subtype, in which, like in thyroid, we found MET, EGFR and ErbB-2 expression and MET–ErbB-2 interactions.

The MET downregulation by siRNA was performed to observe if any alterations occur in either ErbB-2 and/or pERK1/2 expression. Indeed, in both thyroid and breast carcinoma-derived cell lines, it was observed an increase in ErbB-2 expression by Western blot, with the exception of SkBr3 cell line possibly due to the fact that this cell line has ErbB-2 overexpression and subsequently the variation of the protein expression was not detectable by this technique. However, the increase of ErbB-2 expression upon downregulation of MET was detected by PLA where the ErbB-2 homodimers were found in higher number than in cells without treatment. The MAPK pathway was found not to be altered with the downregulation of MET, since no effect was observed in either pErk1/2 or in Erk 1/2 expression by Western blot. In Shattuck *et al.*, 2008, they observed that when ErbB-2 was inhibited with Trastuzumab, a significant increase in MET expression occurred. These, although mirroring our results, are consistent with our observations of the increase expression of ErbB-2 when MET was downregulated. Taking together, they suggest that a kind of cross-talk at the expression level seems to exist between both receptors that deserve further exploration. They also observed that with MET downregulation both MAPK and PI3K/AKT pathways diminished downstream signalling. As previously discussed we couldn't see these results in our experiments towards MAPK pathway, and we did not study PI3K/AKT pathway.

The PLA results from the MET downregulation showed that, while the MET–MET interactions decreased due to its downregulation, the number of interactions MET–ErbB-2 and ErbB-2–ErbB-2 slightly increased in TPC-1 and SkBr3 cell lines. A possible explanation for these results is a competitive RTKs dimer formation model. It is known that both ErbB-2 and MET dimerize with others RTKs like EGFR and ErbB-3. If the receptors compete for the formation of dimers it is possible that when a RTK is downregulated, like MET, the others RTKs, like ErbB-2, which the expression was increased with the downregulation of MET, will compete with the existing MET and form heterodimers instead of homodimers, since ErbB-2 is available in higher number.

Further investigation is necessary to understand the dimers formation, the underlying mechanisms of these interactions, if they are functionally active, and their role in cell stimulation.

After the *in vitro* analysis, an *in vivo* study was performed in a series of invasive breast carcinomas.

From the analysis of the immunohistochemistry results in breast tumours we have observed that MET is not randomly expressed within the tumours, it is significantly associated with some clinicopathological factors like grade, molecular subtype, ER negative and ErbB-2 positive expression. MET expression is increased in high grade tumours since we observed MET expression in 66.7% in grade III tumours in opposition to 35.5% in grade I. Similar results were observed in the relation between MET and molecular subtypes. The expression of MET is inversely related to the expression of ER, which is associated to the Luminal subtype, where only 35% of the cases expressed MET. The Luminal subtype is known to express ER and to be the less aggressive breast cancer subtype. According to the association between MET expression and higher aggressiveness of the tumours, we found co-expression of MET in 75% of the ErbB-2 OE cases, being the association between MET and ErbB-2 the exact opposite of MET and ER.

In the literature MET was already related to an adverse outcome in breast cancer patients (Kang *et al.*, 2003; Ocal *et al.*, 2003; Lengyel *et al.*, 2005 and Lindemann *et al.*, 2006), but it was never related to the established clinicopathological factors.

Our results are in agreement with literature and in addition, we found MET to be significantly associated to other prognosis factors and also with survival, where the Kaplan-Meier analysis of disease-related survival demonstrates that the patients with

tumours expressing MET have a significant lower survival rate. In patients, with Luminal subtype tumours, MET expression is related to a significant poorer survival, which is in accordance to the previous results.

However, we have seen a duality of MET role on survival. Unexpectedly, in patients with ErbB-2 OE subtype the survival was higher when MET was expressed, which might indicate that when the tumours have a highly aggressive behaviour the presence of MET can be predictive for a better patients outcome. Further research is necessary to understand better the effect of MET in the different subtypes of tumours.

In the final part of our study, we considered important to know which prognostic factors were related to the survival of the patients. By univariate analysis we observed that MET, ErbB-2, ER, PR, p63, P-cadherin, grade and age were factors with significant influence on the survival of the patients. Both ER and PR have a significant correlation with a better prognosis of the patients. Indeed, these results are in accordance to the breast cancer subtypes classification, where these receptors expression are correlated with Luminal subtype tumours, which patients have a better clinical outcome. MET, ErbB-2, p63, P-cadherin, grade and age have a significant correlation with a poorer prognosis of the patients, which is according to the previous results and literature. MET, ErbB-2 expression and grade are related to a patients poorer clinical outcome, p63 is a factor associated with metaplastic carcinomas (Koker and Kleer, 2004) and P-cadherin expression is associated with tumour aggressiveness (Paredes *et al.*, 2005).

By multivariate analysis MET was the only clinicopathological factor that remained significant ($P=0.041$). This result indicates that MET, independently of the other prognosis factors, can identify a subset of patients with an adverse outcome of the disease, confirming the previous data and literature.

All these results indicate that the presence of MET is related to a worse prognosis of the patients, and that the association and interactions between MET and ErbB-2 are important to consider. This study leads to the hypothesis that targeting MET alone or with ErbB-2 may be very important in the treatment of breast cancer.

Conclusions

In this study we have observed MET, ErbB-2 and EGFR expression in both thyroid and breast carcinomas-derived cell lines, and demonstrated by Co-IP and PLA techniques MET–ErbB-2 physical interaction in all the cell lines. We have also observed an increase in ErbB-2 expression upon MET downregulation, suggesting a transcriptional cross-talk between expression levels of the two RTKs. Further studies on the role of MET–ErbB-2 interaction on cell biology are essential.

In breast tumours we have demonstrated that MET expression is an independent prognostic factor related to a general poorer survival of the patients, which is clearly associated with other important prognosis factors such as ErbB-2, ER, grade and subtypes. Unexpectedly MET expression seems to exert a protective behaviour on survival of patients with ErbB-2 OE tumours subtype, if confirmed in a larger series this can be an important matter for further investigation.

Taken together, our data has showed an interesting cross-communication between MET and ErbB-2 RTKs in both thyroid and breast carcinomas, which might be helpful for the design of new targeted therapies.

References

- Agarwal, S., Zerillo, C., Kolmakova, J., Christensen, J.G., Harris, L.N., Rimm, D.L., Digiovanna, M.P. & Stern, D.F. (2009). Association of constitutively activated hepatocyte growth factor receptor (Met) with resistance to a dual EGFR/Her2 inhibitor in non-small-cell lung cancer cells. *Br J Cancer*, **100**, 941-9.
- Baselga, J. & Norton, L. (2002). Focus on breast cancer. *Cancer Cell*, **1**, 319-22.
- Bergstrom, J.D., Westermarck, B. & Heldin, N.E. (2000). Epidermal growth factor receptor signalling activates met in human anaplastic thyroid carcinoma cells. *Exp Cell Res*, **259**, 293-9.
- Bhargava, R., Gerald, W.L., Li, A.R., Pan, Q., Lal, P., Ladanyi, M. & Chen, B. (2005). EGFR gene amplification in breast cancer: correlation with epidermal growth factor receptor mRNA and protein expression and HER-2 status and absence of EGFR-activating mutations. *Mod Pathol*, **18**, 1027-33.
- Blume-Jensen, P. & Hunter, T. (2001). Oncogenic kinase signalling. *Nature*, **411**, 355-65.
- Bonine-Summers, A.R., Aakre, M.E., Brown, K.A., Arteaga, C.L., Pietenpol, J.A., Moses, H.L. & Cheng, N. (2007). Epidermal growth factor receptor plays a significant role in hepatocyte growth factor mediated biological responses in mammary epithelial cells. *Cancer Biol Ther*, **6**, 561-70.
- Bublil, E.M. & Yarden, Y. (2007). The EGF receptor family: spearheading a merger of signaling and therapeutics. *Curr Opin Cell Biol*, **19**, 124-34.
- Chan, S.K., Hill, M.E. & Gullick, W.J. (2006). The role of the epidermal growth factor receptor in breast cancer. *J Mammary Gland Biol Neoplasia*, **11**, 3-11.

- Christensen, J.G., Burrows, J. & Salgia, R. (2005). c-Met as a target for human cancer and characterization of inhibitors for therapeutic intervention. *Cancer Lett*, **225**, 1-26.
- Dancey, J.E. & Freidlin, B. (2003). Targeting epidermal growth factor receptor-are we missing the mark? *Lancet*, **362**, 62-4.
- DeLellis R, Lloyd R, Heitz P, Eng C. (2004). World Health Organization of Tumours. Pathology and Genetics: Tumours of endocrine organs. *IARC Press*; 49-91.
- DeLellis, R.A. (2006). Pathology and genetics of thyroid carcinoma. *J Surg Oncol*, **94**, 662-9.
- Di Renzo, M.F., Olivero, M., Martone, T., Maffe, A., Maggiora, P., Stefani, A.D., Valente, G., Giordano, S., Cortesina, G. & Comoglio, P.M. (2000). Somatic mutations of the MET oncogene are selected during metastatic spread of human HNSC carcinomas. *Oncogene*, **19**, 1547-55.
- Ensinger, C., Spizzo, G., Moser, P., Tschöerner, I., Prommegger, R., Gabriel, M., Mikuz, G. & Schmid, K.W. (2004). Epidermal growth factor receptor as a novel therapeutic target in anaplastic thyroid carcinomas. *Ann N Y Acad Sci*, **1030**, 69-77.
- Freudenberg, L.S., Sheu, S., Gorges, R., Mann, K., Bokler, S., Frilling, A., Schmid, K.W., Bockisch, A. & Otterbach, F. (2005). Prognostic value of c-erbB-2 expression in papillary thyroid carcinoma. *Nuklearmedizin*, **44**, 179-82, 184.
- Garcia, S., Dales, J.P., Jacquemier, J., Charafe-Jauffret, E., Birnbaum, D., Andrac-Meyer, L., Lavaut, M.N., Allasia, C., Carpentier-Meunier, S., Bonnier, P. & Charpin-Taranger, C. (2007). c-Met overexpression in inflammatory breast carcinomas: automated quantification on tissue microarrays. *Br J Cancer*, **96**, 329-35.

- Gumurdulu, D., Uguz, A., Erdogan, S., Tuncer, I. & Demircan, O. (2003). Expression of c-erbB-2 oncoprotein in different types of thyroid tumors: an immunohistochemical study. *Endocr Res*, **29**, 465-72.
- Guo, A., Villen, J., Kornhauser, J., Lee, K.A., Stokes, M.P., Rikova, K., Possemato, A., Nardone, J., Innocenti, G., Wetzel, R., Wang, Y., MacNeill, J., Mitchell, J., Gygi, S.P., Rush, J., Polakiewicz, R.D. & Comb, M.J. (2008). Signaling networks assembled by oncogenic EGFR and c-Met. *Proc Natl Acad Sci U S A*, **105**, 692-7.
- Gusterson, B. (2009). Do 'basal-like' breast cancers really exist? *Nat Rev Cancer*, **9**, 128-34.
- Hynes, N.E. & Lane, H.A. (2005). ERBB receptors and cancer: the complexity of targeted inhibitors. *Nat Rev Cancer*, **5**, 341-54.
- Ivan, M., Bond, J.A., Prat, M., Comoglio, P.M. & Wynford-Thomas, D. (1997). Activated ras and ret oncogenes induce over-expression of c-met (hepatocyte growth factor receptor) in human thyroid epithelial cells. *Oncogene*, **14**, 2417-23.
- Kang, J.Y., Dolled-Filhart, M., Ocal, I.T., Singh, B., Lin, C.Y., Dickson, R.B., Rimm, D.L. & Camp, R.L. (2003). Tissue microarray analysis of hepatocyte growth factor/Met pathway components reveals a role for Met, matriptase, and hepatocyte growth factor activator inhibitor 1 in the progression of node-negative breast cancer. *Cancer Res*, **63**, 1101-5.
- Kapp, A.V., Jeffrey, S.S., Langerod, A., Borresen-Dale, A.L., Han, W., Noh, D.Y., Bukholm, I.R., Nicolau, M., Brown, P.O. & Tibshirani, R. (2006). Discovery and validation of breast cancer subtypes. *BMC Genomics*, **7**, 231.
- Koker, M.M. & Kleer, C.G. (2004). p63 expression in breast cancer: a highly sensitive and specific marker of metaplastic carcinoma. *Am J Surg Pathol*, **28**, 1506-12.

- Krauss G. Biochemistry of signal transduction and regulation. (2003) Third, completely revised edition. *WILEY-VCH*.
- Kremser, R., Obrist, P., Spizzo, G., Erler, H., Kendler, D., Kemmler, G., Mikuz, G. & Ensinger, C. (2003). Her2/neu overexpression in differentiated thyroid carcinomas predicts metastatic disease. *Virchows Arch*, **442**, 322-8.
- Lengyel, E., Prechtel, D., Resau, J.H., Gauger, K., Welk, A., Lindemann, K., Salanti, G., Richter, T., Knudsen, B., Vande Woude, G.F. & Harbeck, N. (2005). C-Met overexpression in node-positive breast cancer identifies patients with poor clinical outcome independent of Her2/neu. *Int J Cancer*, **113**, 678-82.
- Liga Portuguesa Contra o Cancro [Internet]. [Cited 2009 April 13]. Available from: <http://www.ligacontracancro.pt>
- Lindemann, K., Resau, J., Nahrig, J., Kort, E., Leeser, B., Annecke, K., Welk, A., Schafer, J., Vande Woude, G.F., Lengyel, E. & Harbeck, N. (2007). Differential expression of c-Met, its ligand HGF/SF and HER2/neu in DCIS and adjacent normal breast tissue. *Histopathology*, **51**, 54-62.
- Longati, P., Comoglio, P.M. & Bardelli, A. (2001). Receptor tyrosine kinases as therapeutic targets: the model of the MET oncogene. *Curr Drug Targets*, **2**, 41-55.
- Mass, R.D. (2004). The HER receptor family: a rich target for therapeutic development. *Int J Radiat Oncol Biol Phys*, **58**, 932-40.
- Menard, S., Pupa, S.M., Campiglio, M. & Tagliabue, E. (2003). Biologic and therapeutic role of HER2 in cancer. *Oncogene*, **22**, 6570-8.
- Menendez, J.A., Mehmi, I. & Lupu, R. (2006). Trastuzumab in combination with heregulin-activated Her-2 (erbB-2) triggers a receptor-enhanced chemosensitivity effect in the absence of Her-2 overexpression. *J Clin Oncol*, **24**, 3735-46.

- Milanezi, F., Carvalho, S. & Schmitt, F.C. (2008). EGFR/HER2 in breast cancer: a biological approach for molecular diagnosis and therapy. *Expert Rev Mol Diagn*, **8**, 417-34.
- Mitsiades, C.S., Kotoula, V., Poulaki, V., Sozopoulos, E., Negri, J., Charalambous, E., Fanourakis, G., Voutsinas, G., Tseleni-Balafouta, S. & Mitsiades, N. (2006). Epidermal growth factor receptor as a therapeutic target in human thyroid carcinoma: mutational and functional analysis. *J Clin Endocrinol Metab*, **91**, 3662-6.
- Palmieri, D., Bronder, J.L., Herring, J.M., Yoneda, T., Weil, R.J., Stark, A.M., Kurek, R., Vega-Valle, E., Feigenbaum, L., Halverson, D., Vortmeyer, A.O., Steinberg, S.M., Aldape, K. & Steeg, P.S. (2007). Her-2 overexpression increases the metastatic outgrowth of breast cancer cells in the brain. *Cancer Res*, **67**, 4190-8.
- Paredes, J., Albergaria, A., Oliveira, J.T., Jeronimo, C., Milanezi, F. & Schmitt, F.C. (2005). P-cadherin overexpression is an indicator of clinical outcome in invasive breast carcinomas and is associated with CDH3 promoter hypomethylation. *Clin Cancer Res*, **11**, 5869-77.
- Pinkas-Kramarski, R., Lenferink, A.E., Bacus, S.S., Lyass, L., van de Poll, M.L., Klapper, L.N., Tzahar, E., Sela, M., van Zoelen, E.J. & Yarden, Y. (1998). The oncogenic ErbB-2/ErbB-3 heterodimer is a surrogate receptor of the epidermal growth factor and betacellulin. *Oncogene*, **16**, 1249-58.
- Robinson, D.R., Wu, Y.M. & Lin, S.F. (2000). The protein tyrosine kinase family of the human genome. *Oncogene*, **19**, 5548-57.
- Ruco, L.P., Stoppacciaro, A., Ballarini, F., Prat, M. & Scarpino, S. (2001). Met protein and hepatocyte growth factor (HGF) in papillary carcinoma of the thyroid: evidence for a pathogenetic role in tumourigenesis. *J Pathol*, **194**, 4-8.

- Schiff, B.A., McMurphy, A.B., Jasser, S.A., Younes, M.N., Doan, D., Yigitbasi, O.G., Kim, S., Zhou, G., Mandal, M., Bekele, B.N., Holsinger, F.C., Sherman, S.I., Yeung, S.C., El-Naggar, A.K. & Myers, J.N. (2004). Epidermal growth factor receptor (EGFR) is overexpressed in anaplastic thyroid cancer, and the EGFR inhibitor gefitinib inhibits the growth of anaplastic thyroid cancer. *Clin Cancer Res*, **10**, 8594-602.
- Shattuck, D.L., Miller, J.K., Carraway, K.L., 3rd & Sweeney, C. (2008). Met receptor contributes to trastuzumab resistance of Her2-overexpressing breast cancer cells. *Cancer Res*, **68**, 1471-7.
- Soares, P., Sambade, C. & Sobrinho-Simoes, M. (1994). Expression of C-erb B2 in tumours and tumour-like lesions of the thyroid. *Int J Cancer*, **56**, 459-61.
- Soderberg, O., Gullberg, M., Jarvius, M., Ridderstrale, K., Leuchowius, K.J., Jarvius, J., Wester, K., Hydbring, P., Bahram, F., Larsson, L.G. & Landegren, U. (2006). Direct observation of individual endogenous protein complexes in situ by proximity ligation. *Nat Methods*, **3**, 995-1000.
- Stephens, P., Hunter, C., Bignell, G., Edkins, S., Davies, H., Teague, J., Stevens, C., O'Meara, S., Smith, R., Parker, A., Barthorpe, A., Blow, M., Brackenbury, L., Butler, A., Clarke, O., Cole, J., Dicks, E., Dike, A., Drozd, A., Edwards, K., Forbes, S., Foster, R., Gray, K., Greenman, C., Halliday, K., Hills, K., Kosmidou, V., Lugg, R., Menzies, A., Perry, J., Petty, R., Raine, K., Ratford, L., Shepherd, R., Small, A., Stephens, Y., Tofts, C., Varian, J., West, S., Widaa, S., Yates, A., Brasseur, F., Cooper, C.S., Flanagan, A.M., Knowles, M., Leung, S.Y., Louis, D.N., Looijenga, L.H., Malkowicz, B., Pierotti, M.A., Teh, B., Chenevix-Trench, G., Weber, B.L., Yuen, S.T., Harris, G., Goldstraw, P., Nicholson, A.G., Futreal, P.A., Wooster, R. & Stratton, M.R. (2004). Lung cancer: intragenic ERBB2 kinase mutations in tumours. *Nature*, **431**, 525-6.

- Ocal, T. I., Dolled-Filhart, M., D'Aquila, T.G., Camp, R.L. & Rimm, D.L. (2003). Tissue microarray-based studies of patients with lymph node negative breast carcinoma show that met expression is associated with worse outcome but is not correlated with epidermal growth factor family receptors. *Cancer*, **97**, 1841-8.
- Utrilla, J.C., Martin-Lacave, I., San Martin, M.V., Fernandez-Santos, J.M. & Galera-Davidson, H. (1999). Expression of c-erbB-2 oncoprotein in human thyroid tumours. *Histopathology*, **34**, 60-5.
- Wasenius, V.M., Hemmer, S., Karjalainen-Lindsberg, M.L., Nupponen, N.N., Franssila, K. & Joensuu, H. (2005). MET receptor tyrosine kinase sequence alterations in differentiated thyroid carcinoma. *Am J Surg Pathol*, **29**, 544-9.
- Weigelt, B., Horlings, H.M., Kreike, B., Hayes, M.M., Hauptmann, M., Wessels, L.F., de Jong, D., Van de Vijver, M.J., Van't Veer, L.J. & Peterse, J.L. (2008). Refinement of breast cancer classification by molecular characterization of histological special types. *J Pathol*, **216**, 141-50.
- Willmore-Payne, C., Holden, J.A. & Layfield, L.J. (2006). Detection of epidermal growth factor receptor and human epidermal growth factor receptor 2 activating mutations in lung adenocarcinoma by high-resolution melting amplicon analysis: correlation with gene copy number, protein expression, and hormone receptor expression. *Hum Pathol*, **37**, 755-63.
- Yarden, Y. & Sliwkowski, M.X. (2001). Untangling the ErbB signalling network. *Nat Rev Mol Cell Biol*, **2**, 127-37.

Annexe I

Solutions used in Material and Methods

Wash Buffers

- Phosphate Buffered Saline – PBS 10x

To prepare 1L add 80g of Sodium chloride (NaCl), 2g of Potassium chloride (KCl), 14.4g of Sodium phosphate dibasic (Na_2HPO_4) and 2.4g of Potassium phosphate monobasic (KH_2PO_4) to 1L of ddH₂O. Adjust pH to 7.4 and store at room temperature.

- PBS1x 0.02% Tween 20

To prepare 1L add 100mL of 10x PBS to 900mL of ddH₂O, 20μL of Tween 20 and mix. Store at room temperature.

- Salt Sodium Citrate – SSC 20x

Dissolve 17.5g NaCl and 8.8g Sodium citrate ($\text{Na}_3\text{C}_3\text{H}_5\text{O}(\text{COO})_3$) into 1L ddH₂O. Adjust pH to 7.0. Filter the solution through a 0.22 μm filter and store at +4°C.

- Tris Buffered Saline – TBS Tween 20

Dissolve 8.8g NaCl, 1.2g Tris base and 0.5 ml Tween 20 into 1L ddH₂O. Adjust pH to 7.4. Filter the solution through a 0.22 μm filter and store at +4°C.

Protein extraction

- Ripa lysis buffer

Add 50mM Tris-HCl, 1%NP-40, 150mM NaCl and 2mM EDTA into ddH₂O. Adjust pH to 7.5 and store at 4°C. Before use add 1% fosfatases' inhibitor and 7% proteases' inhibitor in PBS.

Co-Immunoprecipitation

- Catenin Lysis Buffer

Add 1% Triton X-100, 1% NP40 in PBS1x.

- Buffer C

For 50ml final volume add 5ml of Catenin Lysis Buffer, 250mg Sodium diphosphate (Na₄P₂O₇), 0.5ml Sodium fluoride (NaF) in the total volume of PBS1x.

Immunohistochemistry

- Peroxidase Inhibition

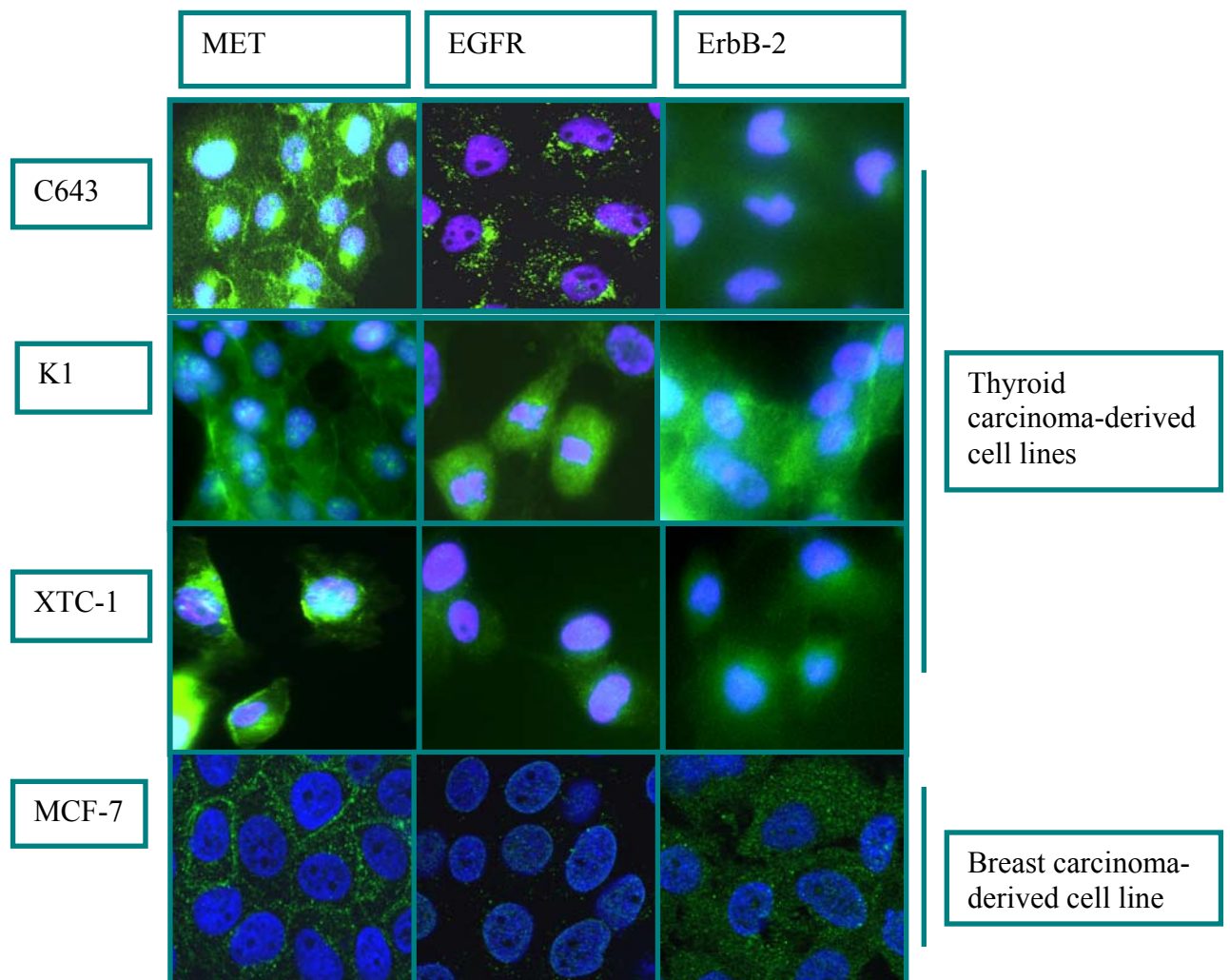
- 3% v/v Hydrogen Peroxide

To prepare approximately 2 mL, add 200μL of 30% Hydrogen peroxide (H₂O₂) to 2mL of methanol (CH₃OH). Notice that this solution has to be prepared a few moments before being used.

Annexe II

Characterization of MET, EGFR and ErbB-2 expression, obtained by Immunofluorescence and Western Blot, in C643, K1, XTC-1 and MCF-7 cells lines.

Immunofluorescence



Western Blot

